nature medicine

Article

https://doi.org/10.1038/s41591-026-04221-z

Transmission dynamics of Oropouche virus in Latin America and the Caribbean

Received: 3 September 2025

Accepted: 13 January 2026

Published online: 24 March 2026

Check for updates

A list of authors and their affiliations appears at the end of the paper

Oropouche virus (OROV) is an arbovirus endemic to the Amazon region since the 1950s that re-emerged in late 2023, causing a major epidemic across Central and South America. Here we investigated the transmission dynamics of the 2023–2024 epidemic in Manaus City (Amazonas state, Brazil), a major metropolitan hub in the Amazon, and estimated OROV infections across Latin America and the Caribbean. OROV re-emergence in Manaus resulted in an increase of IgG seroprevalence from 11.4% in November 2023 to 25.7% in November 2024. The neutralizing capacity of OROV-specific IgG antibodies from individuals collected before and after the re-emergence demonstrated a median plaque reduction neutralization test 50% titer of 640 against both the historical and contemporary OROV isolates. A historical reconstruction of OROV circulation in Manaus indicated a continuous low-level transmission with two major outbreaks of comparable seasonality and magnitude in 1980–1981 and 2023–2024. We estimate approximately 336,000 OROV infections in the Amazon region under a scenario of continuous endemic transmission without major outbreaks and over 9.4 million OROV infections during major outbreaks from 1960 to 2025. Collectively, our findings provide a comprehensive assessment of OROV transmission in Manaus and contribute to a better understanding of the OROV burden.

Oropouche virus (OROV) is a neglected arbovirus that has caused Oropouche fever in Latin America and the Caribbean since the 1950s[1,2]. Oropouche fever is a febrile illness that is often mild and self-limited[1,3]. However, OROV infection in some patients can lead to central nervous system diseases (for example, meningitis and meningoencephalitis), maternal–fetal complications (for example, stillbirths and birth defects) and death[1,3–5]. OROV is primarily transmitted to humans by the bite of *Culicoides paraensis* midges, sometimes called 'no-see-ums' in enzootic and urban cycles[1]. In the enzootic cycle, pale-throated sloths (*Bradypus tridactylus*) and nonhuman primates can serve as host reservoirs[1]. As of October 2025, no antiviral drugs or vaccines are available for the treatment or prevention of OROV infection.

OROV is classified into the species *Orthobunyavirus oropoucheense* in the *Orthobunyavirus* genus of the *Peribunyaviridae* family[6]. Its genome consists of three single-stranded, negative-sense RNA molecules, designated as small, medium and large segments[6]. OROV can undergo reassortment events when two related orthobunyaviruses infect the same cell[7]. These events generate novel viral strains with mixed genomic segments from both parent strains, such as those described for Iquitos, Madre de Dios and Perdões viruses[8–10]. Reassortment is a key evolutionary mechanism because it increases viral genetic diversity and may affect vector competence, immunogenicity and disease severity[11].

Since late 2023, the incidence of Oropouche fever has increased in the Brazilian Amazon region, with subsequent spread to all 26 Brazilian states and the Federal District[12,13]. Between 2024 and 2025, autochthonous OROV transmission has also been reported in Barbados, Bolivia, Colombia, Cuba, the Dominican Republic, Ecuador, Guyana, Panama, Peru and Venezuela[14–19]. In addition, travel-related cases have been reported in Canada, the Cayman Islands, Germany, Italy, Spain and the USA[20,21]. This re-emergence of OROV has been associated with a novel OROV reassortant that may have higher fitness and virulence

e-mail: jlmodena@unicamp.br; sabinoec@usp.br; wmdesouza@uky.edu

https://doi.org/10.1038/s41591-026-04221-z

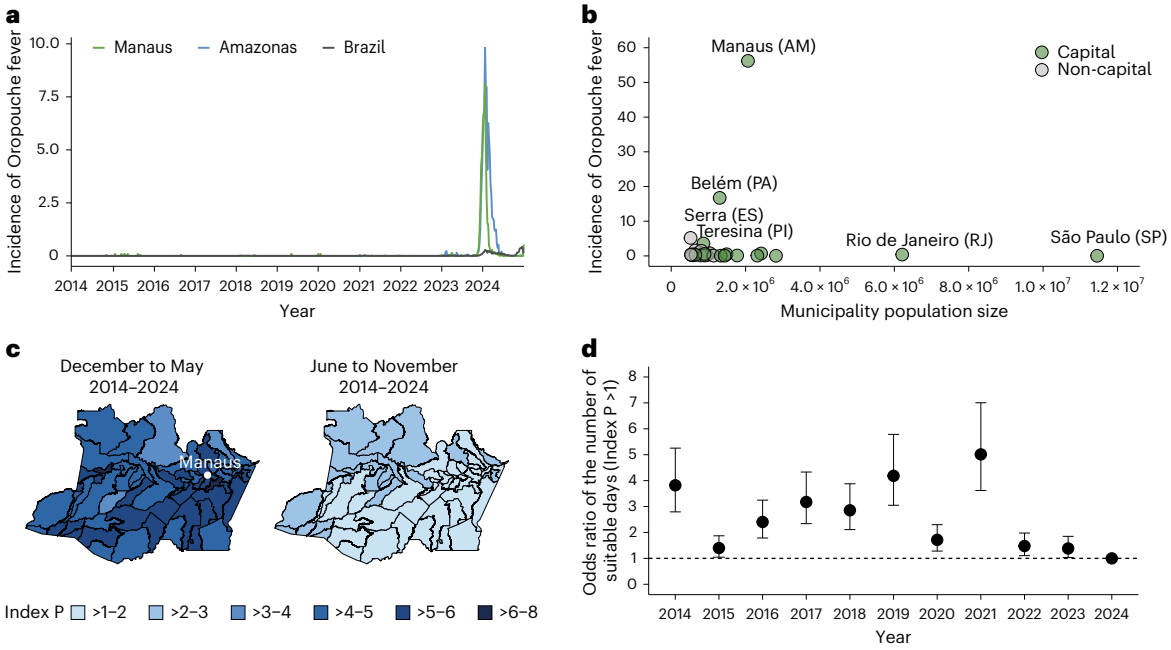

Fig. 1 | Oropouche fever outbreak in Manaus, 2023–2024. a, The incidence of Oropouche fever laboratory-confirmed cases per epidemiological week in Manaus, Amazonas state, and Brazil, from epidemiological week 1 of 2014 (29 December to 4 January) to epidemiological week 52 of 2024 (22–28 December). **b**, The incidence of Oropouche fever in Brazilian municipalities with a population of ≥500,000 inhabitants (n = 29). **c**, The mean monthly Index P for OROV transmission by *C. paraensis* between 2014 and 2024 in Amazonas state during the wet season (December to May) compared to the dry season (June to November) at the municipality level. The mean monthly Index P data for all months in Amazonas state are shown in Extended Data Fig. 1. Index P ≥ 1 indicates a suitable climate and Index P < 1 indicates an unsuitable climate. **d**, Odds ratios for the number of days suitable for OROV transmission (defined as Index P > 1) in each year from 2014 to 2023 compared to 2024 (the reference year). The dots represent the odds ratio and bars indicate the 95% CIs. Brazilian states: AM, Amazonas state; ES, Espírito Santo state; PA, Pará state; PI, Piauí state; RJ, Rio de Janeiro state; SP, São Paulo state. Shapefile in **c** from the Instituto Brasileiro de Georgrafia e Estatística under a Creative Commons license CC BY 4.0.

compared to previous OROV strains and may be able to evade antibody responses generated by prior OROV infections[12,22]. Furthermore, anthropogenic factors, including land use, land cover and human mobility, are likely contributors to facilitated OROV re-emergence in the Amazon region[13,23]. The combination of OROV-infected travelers, widespread distribution of *C. paraensis* across the Americas and a large, immunologically naive population may have contributed to the establishment of OROV transmission beyond the Amazon region.

The Amazon region has approximately 47 million inhabitants across Brazil, Peru, Colombia, Bolivia, Ecuador, French Guiana, Guyana, Suriname and Venezuela. This region is characterized by a low population density (ranging from 1.8 to 19 inhabitants per square kilometer) and a high level of deforestation[24]. Manaus City (Amazonas State, Brazil) is the largest metropolis in the Amazon, with a population of approximately 2.27 million and a density of 181 inhabitants per square kilometer, and was the first major urban center affected by the 2023–2024 OROV re-emergence before its broader spread beyond the Amazon Basin[13]. In this study, we combined epidemiological, ecological, serological and serodynamic analyses to investigate OROV transmission dynamics in Manaus and estimate the number of OROV infections in Latin America and the Caribbean.

Results

Oropouche fever re-emergence in Manaus between 2023 and 2024

Between 1 January 2014 and 31 December 2024, Manaus, the capital and largest city of Amazonas state, reported 1,160 laboratory-confirmed Oropouche fever cases to the Brazilian Ministry of Health (Fig. 1a). The majority of these cases (96.3%, 1,117 of 1,160) occurred between 1 December 2023 and 30 June 2024. The cumulative incidence was 54.1 cases per 100,000 inhabitants in Manaus, which was 12.7 times higher than the cumulative Oropouche fever incidence at the national level during the same period. Notably, Manaus exhibited the highest cumulative OROV incidence among all Brazilian municipalities with over 500,000 inhabitants (n = 29; Fig. 1b). We estimated the OROV laboratory positivity rate in Manaus to be 12.2% (95% confidence interval (CI) 11.5–12.9%). This rate was estimated to be 1.2 times lower than across Amazonas state (14.9%, 95% CI 14.5–15.4%) but 1.5 times higher than the national average (8.3%, 95% CI 8.2–8.4%) (Extended Data Fig. 1). The median age of Oropouche fever cases in Manaus was 35 years (interquartile range 24–48 years) and 53.1% (616 of 1,160) of cases were male. To investigate the impact of climate on the OROV primary vector, we examined the climate suitability (Index P) for *C. paraensis* between January 2014 and December 2024 (Extended Data Table 1). We found that Amazonas state has a climate suitable for *C. paraensis* throughout the year, with the highest suitability during the wet season from December to May (Index P ≥ 6.53) and lowest during the dry season between June and November (Index P ≥ 2.94; Fig. 1c and Extended Data Fig. 2). This period of high seasonal suitability in Manaus (December to May) consistently overlaps with the increase in Oropouche fever cases in late 2023 and early 2024. However, we found that the number of days with climate suitability for *C. paraensis* in 2023 and 2024 was not statistically higher than the 9 years preceding the re-emergence (Fig. 1d and Extended Data Fig. 3).

OROV seroprevalence in Manaus

To determine the seroprevalence of OROV infections in Manaus, we conducted a cross-sectional seroepidemiological study using 2,055 routine blood donor samples. Samples were collected in three distinct periods: November 2023 (n = 685), June 2024 (n = 685) and November 2024 (n = 685). Of the total samples, 98.9% (n = 2,033) were from unique individuals and 1.1% (n = 22) represented repeat donors. The mean age

https://doi.org/10.1038/s41591-026-04221-z

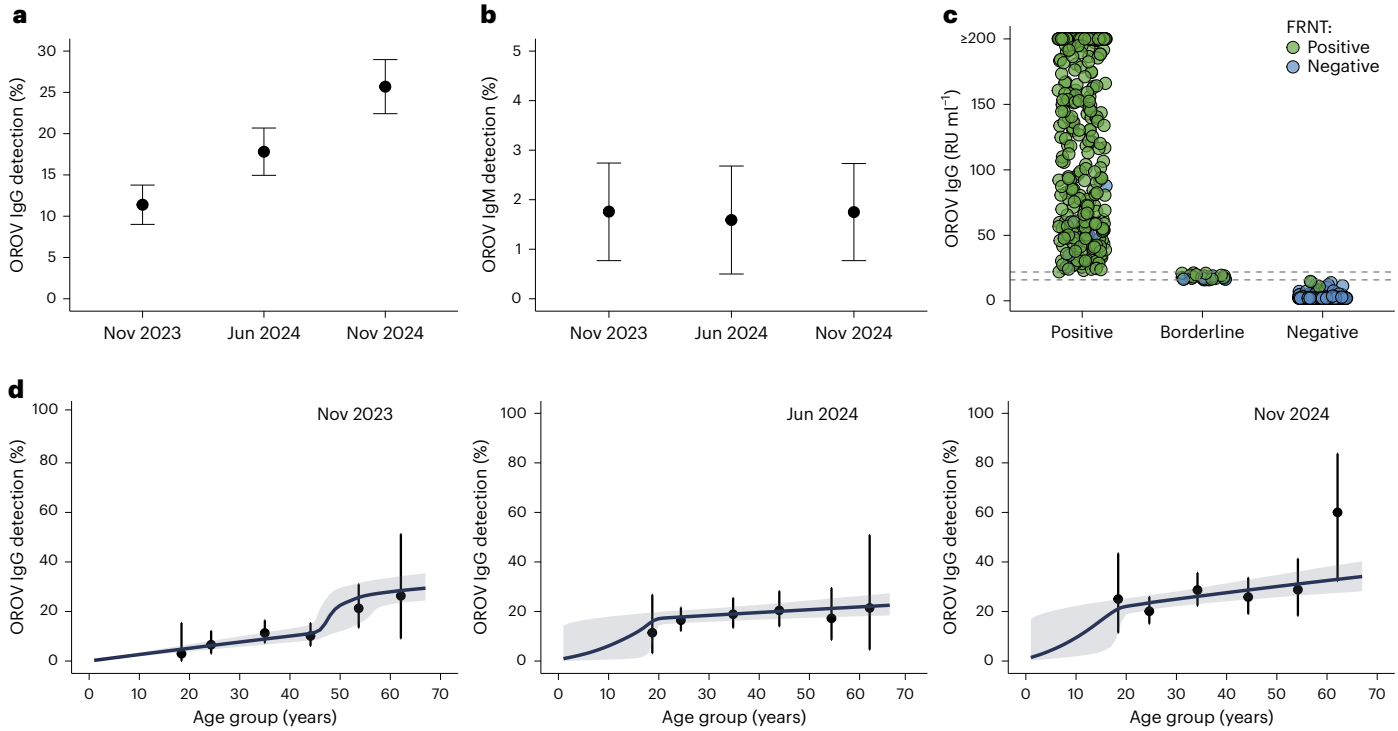

Fig. 2 | Detection of OROV-specific antibodies in Manaus between 2023 and 2024. a, OROV IgG seropositivity rate by sampling period. Seropositivity rates are shown for three time points (November (Nov) 2023, June (Jun) 2024 and Nov 2024) among individuals aged 16–69 years (n = 685 per period). The dots represent observed seroprevalence and error bars indicate 95% CIs. **b**, OROV IgM seropositivity rate by sampling period. Seropositivity rates are shown for three time points among individuals aged 16–69 years: Nov 2023 (n = 683), Jun 2024 (n = 504) and Nov 2024 (n = 685). The dots represent observed seroprevalence and error bars indicate 95% CIs. **c**, The agreement between IgG ELISA and FRNT (n = 630). The upper dashed line indicates the cutoff for IgG positive (≥22 RU ml^{-1}), while the lower dashed line indicates IgG negative (<16 RU ml^{-1}) as established by the manufacturers. The area between the two dashed lines represents the borderline range (≥16 to <22 RU ml^{-1}). **d**, Age-stratified OROV-specific IgG seroprevalence in Manaus across three sampling periods: Nov 2023, Jun 2024 and Nov 2024. The posterior distribution of the catalytic model fitted seroprevalence for each age is represented as posterior mean (dark blue) and 95% credible intervals (shaded gray). The dots represent the observed seroprevalence and bars indicate the 95% CIs. Seropositivity rates are shown for three time points (Nov 2023, Jun 2024 and Nov 2024) among individuals aged 16–69 years (n = 685 per period).

of participants was 36 years (interquartile range 26–44 years), with males comprising 68.7% (1,412 of 2,055) and females 31.3% (643 of 2,055) of the samples. OROV IgG seroprevalence was 11.4% (78 of 685, 95% CI 9.1–14.0%) in November 2023. This rate increased to 17.8% (122 of 685, 95% CI 15.0–20.9%) in June 2024 and reached 25.7% (176 of 685, 95% CI 22.5–29.1%) by November 2024 (Fig. 2a). By contrast, the OROV IgM seropositivity rate was 1.8% (12 of 683, 95% CI 0.8–2.74) in November 2023, 1.6% (8 of 504, 95% CI 0.5–2.68) in June 2024 and 1.8% (12 of 685, 95% CI 0.8–2.73) in November 2024 (Fig. 2b). To confirm the robustness of the enzyme-linked immunosorbent assay (ELISA) used, a subset of IgG ELISA-positive samples (n = 325), IgG ELISA-negative samples (n = 274) and all IgG ELISA-borderline samples (n = 31) were tested using a focus reduction neutralization test (FRNT). The agreement between the ELISA and FNRT was 97.8% (318/325) for IgG-positive samples and 98.5% (270/274) for IgG-negative samples. Furthermore, 77.4% (24 of 31) of the IgG-borderline samples from ELISA were confirmed as OROV positive by FRNT (Fig. 2c). Our age-stratified analysis of OROV IgG-positive samples from November 2023 revealed that individuals aged ≥50 years exhibited seroprevalence rates ranging from 21.3% (95% CI 13.5–30.9%) to 26.3% (95% CI 9.2–51.2%) compared to those aged <50 years with seroprevalence rates ranging from 2.9% (95% CI 0.01–15.3%) to 11.3% (95% CI 7.4–16.4%; Fig. 2d and Extended Data Table 2). However, this age-dependent pattern was not observed in the serosurveys conducted in July and November 2024, which were instead characterized by an increase in seropositivity across all age groups (Fig. 2d). Therefore, the data indicate that most individuals (that is, aged >50 years) who tested seropositive for OROV in November 2023 were probably exposed to the virus in a previous transmission outbreak.

OROV-specific antibodies before and after the 2023–2024 outbreak in Manaus

To further understand the dynamics of humoral OROV immunity, we assessed the neutralizing capacity of OROV IgG and IgM antibodies using the plaque reduction neutralization test 50% ($PRNT_{50}$). We evaluated their ability to neutralize two distinct OROV strains: the prototype BeAn19991 isolate (1960) and the contemporary AM0088 isolate (2024). A subset of samples from OROV IgG-positive individuals collected before and after 2023–2024 was divided into two age groups: ≥50 years old and <50 years old. In serum samples from IgG-positive individuals from both age groups, we found $PRNT_{50}$ titer of ≥640 against the BeAn19991 and AM0088 strains, both before and after the 2023–2024 outbreak (Fig. 3a,b). No statistically significant difference in OROV IgG concentration (relative units (RU) per milliliter) was observed between the two age groups either before or after the outbreak (Fig. 3c). Then, we evaluated the neutralizing antibody capacity of all OROV IgM-positive samples (n = 14) against both OROV strains using $PRNT_{50}$. These samples exhibited a median $PRNT_{50}$ titer of ≥640 for the AM0088 isolate. By contrast, the same serum samples showed $PRNT_{50}$ titers below the detection limit (<20) against the BeAn19991 isolate (Fig. 3d). Among the 22 individuals with repeat blood donations, we identified two who seroconverted from OROV IgG negative to IgG positive, indicating a primary infection between sampling. In addition, an increase in OROV IgG concentration was observed in previously IgG-positive individuals, and one of these individuals also had a positive IgM result in their second donation (Fig. 3e). However, we did not observe any increase in neutralizing capacity in OROV antibody-positive samples (Extended Data Table 3).

Reconstruction of major OROV outbreaks in Manaus

To reconstruct the historical circulation of OROV and contextualize the 11.4% IgG seroprevalence measured in November 2023, we employed a serodynamic approach. Based on a serocatalytic model assuming a constant transmission with a single prior outbreak, fitted to our November 2023 serosurvey data, we estimated that Manaus experienced a major OROV outbreak in mid-1976 (95% Bayesian credible interval: 1966–1978; Fig. 4a). To refine the resolution of our reconstruction, we conducted an additional and retrospective cross-sectional serosurvey between 2015 and 2016 in the general population from Manaus (n = 440 participants). This serosurvey found an OROV seroprevalence of 11.1% (49 of 440, 95% CI 8.4–14.5%), with a median $PRNT_{50}$ titer of 640 (interquartile range 200–640) for the BeAn19991 strain. Consistent with our earlier findings, individuals ≥40 years old exhibited a seroprevalence of at least 19.1% (95% CI 5.5–4.2), while those <40 years old showed a seroprevalence ≤6.1% (95% CI 0.7–20.2) (Fig. 4b). Next, using the 2015–2016 serosurvey data in our serocatalytic model with the same assumptions above, we estimated that a major OROV outbreak occurred in Manaus around 1977 (95% Bayesian credible interval: 1972–1981; Fig. 4c). Our estimate for outbreak reconstruction is supported by historical records of a major OROV outbreak in Amazonas state in 1980, which affected Manaus between October 1980 and February 1981[25] (Extended Data Table 4). The previous study from that period estimated OROV seroprevalence in the Manaus population before the 1980–1981 outbreak at 1.8% (9 of 496), with 4.2% (21 of 496) during the serosurvey in December of 1980, which subsequently rose to 14.9% (74 of 496) post-outbreak (May 1981)[25]. Collectively, our data indicate a sustained but lower level of OROV transmission in Manaus, with infections occurring predominantly during two major outbreaks (that is, 1980–1981 and 2023–2024) that exhibited comparable seasonality and magnitude (Fig. 4d).

Number of OROV infections in Latin America and the Caribbean

To estimate the number of OROV infections in endemic Central and South American countries, we compiled data from major OROV outbreaks and seroepidemiological studies between 1961 and 2022 (Extended Data Table 4 and Supplementary Table 1). We identified 32 major OROV outbreaks documented in Brazil, Peru, French Guiana and Panama, with 59.4% (19 of 32) occurring in Brazil (Fig. 5a). These outbreaks were mostly restricted to the municipality or state level, with a median duration of 2 months (interquartile range 1–3 months). Our analysis identified 187 OROV seroepidemiological studies, predominantly performed in the 1970s (n = 43), 2010s (n = 60) and 2020s (n = 50). The serosurveys conducted in Brazil represent 39.0% (73 of 187) of these studies (Fig. 5b). Then, we categorized the seroepidemiological studies based on whether they were conducted before or after a major OROV outbreak (Supplementary Table 1). We found a significant difference in median OROV seroprevalence: 0.65% (interquartile range 0.00–1.84%, n = 118) before outbreaks compared to 16.7% (interquartile range 9.09–33.74%, n = 69) after outbreaks (P < 0.0001; Fig. 5c). To estimate the number of OROV infections in endemic areas (that is, Amazon Basin), we used the median and interquartile range of seroprevalence from before outbreaks to reflect a scenario of continuous endemic transmission. We estimated 336,570 OROV infections (with 75th percentile: 0.95 million OROV infections) in the Amazon region in the current population, with the highest numbers in Brazil and Peru (Fig. 5d). Using the median and interquartile range of seroprevalence data from after OROV outbreaks, we estimated a cumulative total of 9.4 million OROV infections (interquartile range 5.1–19.0 million) between 1960 and 2025 across Latin America and the Caribbean (Fig. 5e). Brazil accounted for the majority of these infections, with an estimated 5.5 million (interquartile range 3.0–11.1 million), followed by Cuba with 1.7 million (interquartile range 0.93–3.4 million) and Peru with 1.1 million (interquartile range 0.59–2.2 million) infections.

Inequalities in surveillance capacity and healthcare accessibility in OROV endemic areas

To understand the gap between reported cases and our estimated number of OROV infections, we assessed both surveillance capacity and healthcare accessibility in OROV-affected regions by examining historical endemic areas in the Amazon Basin and areas recently affected by the 2024–2025 epidemic. We found that 77.8% (seven of nine) of endemic OROV areas in the Amazon Basin have a median surveillance capability index below the South American median of 0.22 (range 0 is poor and 1 is excellent), including Peru, Colombia and Bolivia, with a median index ranging from 0.04 to 0.21 (Fig. 6a). Brazil and Ecuador showed slightly higher indices of 0.25 (interquartile range 0.21–0.31) and 0.24 (interquartile range 0.08–0.47), respectively. Conversely, countries recently affected by OROV outbreaks in the Caribbean had a higher median index ranging from 0.60 to 0.89 (Fig. 6a). Similarly, our analysis of optimal travel time to healthcare facilities shows substantial differences between endemic and recently affected areas. The median optimal travel time in OROV endemic areas is often long, with a median of 14 to 22.5 h in Peru, Colombia and Venezuela, and a range exceeding 24 h (Fig. 6b). By contrast, the median travel time in Caribbean countries was less than 10 min. The median travel time to healthcare was reduced after the 2023–2025 outbreaks in Brazil and Ecuador, which is probably owing to the geographical expansion of OROV to areas with faster travel times (Fig. 6b). Collectively, these findings show that endemic areas with continuous OROV transmission in the Amazon Basin have a lower surveillance capacity and limited healthcare accessibility, which probably contribute to the underreporting of OROV infections.

Discussion

This study provides a comprehensive assessment of the re-emergence of Oropouche fever in Manaus and the Amazon Basin, which may be critical to understanding the nidus of the 2023–2025 OROV epidemic across Latin America and the Caribbean. Our data show the 2023–2024 OROV outbreak in Manaus led to a significant increase in IgG seroprevalence from 11.4% in November 2023 (pre-outbreak) to 25.7% in November 2024 (post-outbreak), which is similar to areas affected by OROV outbreaks in South America[26]. Notably, our historical reconstruction of OROV circulation indicates that Manaus was affected by a major outbreak

Fig. 3 | OROV antibody response before and after the 2023–2024 outbreak in Manaus. a, Neutralization of OROV strains BeAn19991 (prototype) and AM0088 (contemporary) by $PRNT_{50}$ in serum samples from OROV IgG-positive individuals collected in November 2023 (pre-outbreak) from individuals aged 16–69 years (left, <50 years old (n = 34) and right, ≥50 years old (n = 15)). **b**, Neutralization of OROV strains by $PRNT_{50}$ in serum samples from OROV IgG-positive individuals collected in June and November 2024 (post-outbreak) from individuals aged 16–69 years (left, <50 years old (n = 48) and right, ≥50 years old (n = 22)). **c**, OROV-specific IgG concentration (RU ml^{-1}) determined by ELISA in serum samples from individuals <50 years (n = 53) and ≥50 years (n = 25) collected pre-outbreak (left) and <50 years (n = 257) and ≥50 years (n = 43) collected post-outbreak (right). The bar in the box plots represents the median (middle line), the upper and lower limits represent the 75th and 25th percentiles, and the lowest and highest values within 1.5× IQR from the first and third quartiles (whiskers). The dashed line indicates the cutoff for IgG positivity (≥22 RU ml^{-1}). Samples below the dashed line were confirmed positive by FRNT. The P values (P = 0.2586 and P = 0.2227) were calculated using the two-sided Wilcoxon rank sum test. **d**, $PRNT_{50}$ neutralization of OROV strains BeAn19991 and AM0088 in serum samples from IgM-positive individuals aged 16–69 years (n = 14) collected between November 2023 and November 2024. **e**, IgG concentrations (RU ml^{-1}) determined by ELISA from 22 individuals (aged 16–69 years) with repeat blood donations, with IgM detection status indicated. The dots represent individual patients. The dashed line indicates the cutoff for IgG positivity (≥22 RU ml^{-1}). The lines connect the ELISA results from the first and second samples of each individual subject.

https://doi.org/10.1038/s41591-026-04221-z

between late 1980 and early 1981, which was the first documented in Amazonas state[25]. These two major outbreaks occurred 42 years apart but shared a comparable seasonality with peaks between December and April (wet season) and resulted in similar attack rates with 12.5% in 1980–1981 and 14.3% in 2023–2024. We hypothesize that Manaus, the largest city in the Amazon region, with its high population density and substantial human mobility facilitated by the largest national and international airport in the Amazon Basin, may have served as a hub for the OROV dissemination beyond the Amazon. This hypothesis is supported by previous genomic epidemiological studies that demonstrated that OROV strains sequenced in other Brazilian states and from traveler-related cases share a recent common ancestor with strains from Manaus in early 2024 (refs. 3,13,27). Likewise, air transportation has been linked with the introduction and spread of other arboviruses, including chikungunya (CHIKV), Zika and new lineages and genotypes of dengue viruses nearly worldwide[28–32].

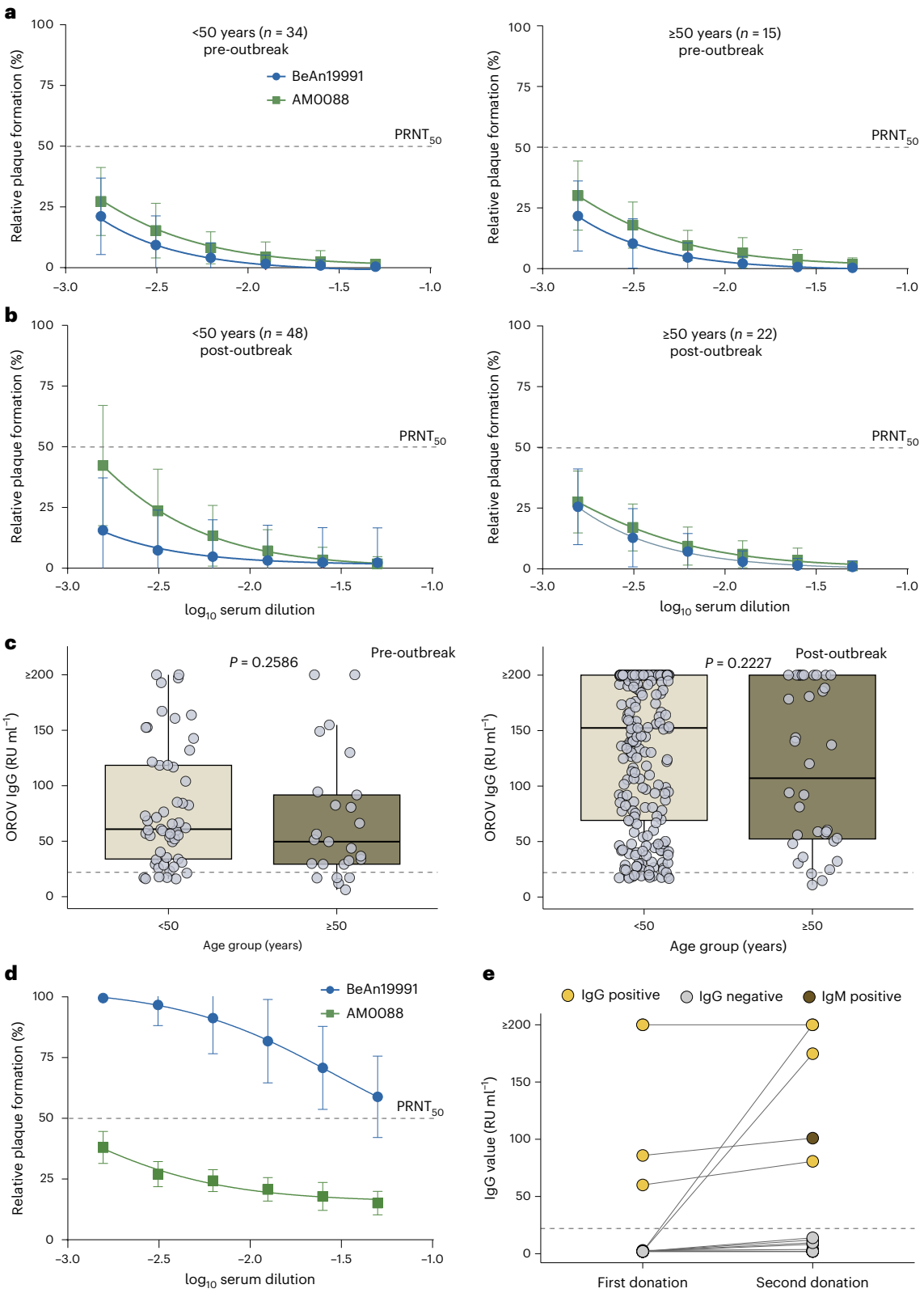

https://doi.org/10.1038/s41591-026-04221-z

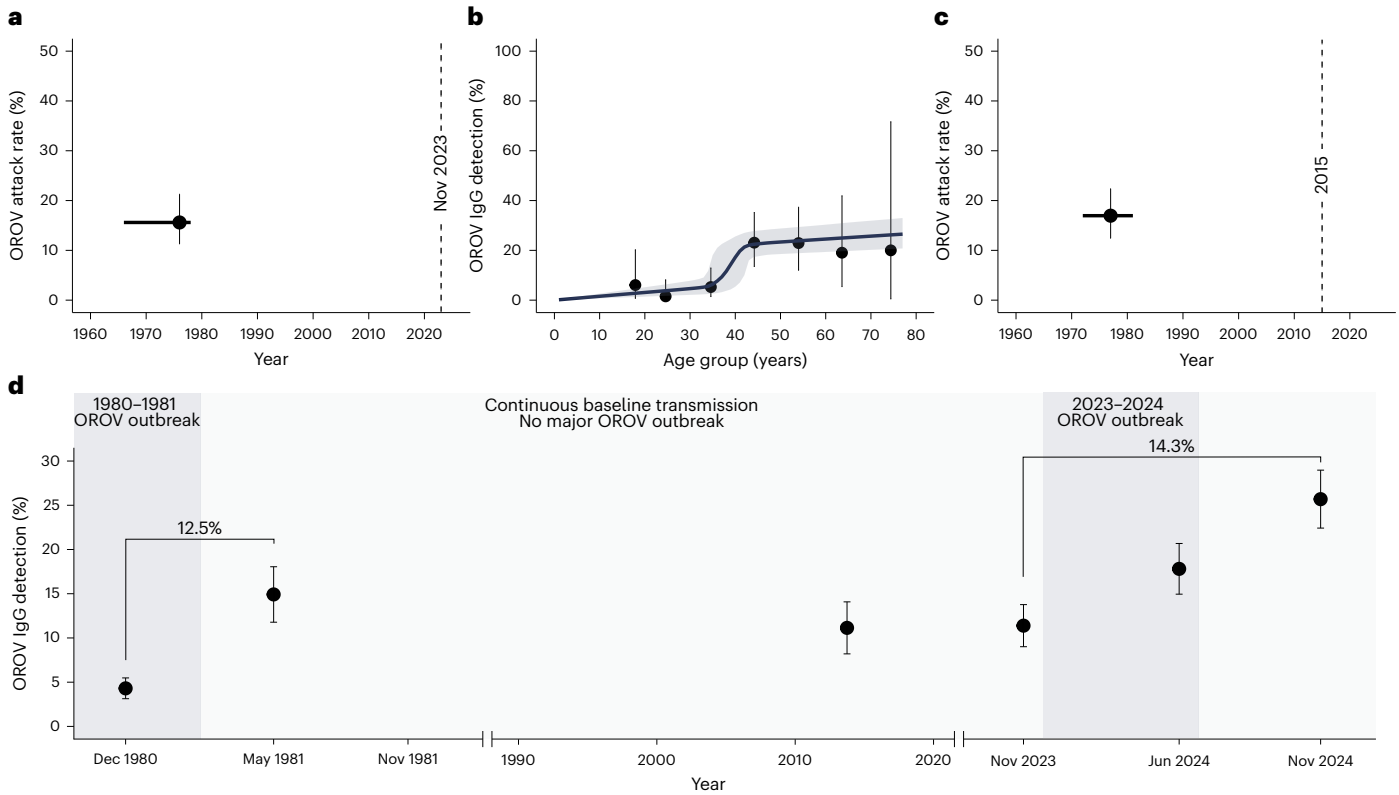

Fig. 4 | Reconstruction of Oropouche fever outbreaks in Manaus. **a**, Posterior distribution of the attack rate and outbreak year from a serocatalytic model, fitted to the November 2023 seroepidemiological data ($n = 685$). The model assumes a constant transmission with a single prior outbreak before November 2023. The dots represent the median of the posterior distribution and lines represent the 95% credible intervals. **b**, Age-stratified OROV-specific IgG seroprevalence in Manaus based on serosurvey data from 2015 to 2016 ($n = 314$), with individuals aged 14–77 years. Data are represented as observed seroprevalences (dots) with 95% CIs (bars). The posterior distribution of the model fitted seroprevalence for each age is represented as posterior mean (dark blue) and 95% credible intervals (gray ribbon). **c**, Posterior distribution of the attack rate and outbreak year from the same serocatalytic model assuming constant transmission with a single prior outbreak before 2015, fitted to the 2015–2016 seroepidemiological data ($n = 314$). The dots represent the median of the posterior distribution and lines represent the 95% credible intervals. **d**, A conceptual representation of the reconstructed history of Oropouche fever outbreaks in Manaus from 1980 to 2024. The figure integrates model predictions with documented historical and recent outbreaks to visualize the temporal dynamics of OROV transmission. Data from the 1980–1981 OROV outbreak in Manaus were obtained from a previous study[25]. The dots represent the observed seroprevalence and bars indicate the 95% CIs.

Our in vitro data indicate that OROV-specific IgG antibodies from individuals previously infected in Manaus can efficiently neutralize both the prototype OROV strain and the representative strain that caused the 2023–2024 outbreak in Manaus. Despite the currently uncertain duration of OROV-specific IgG antibody responses, our reconstruction of the 1980–1981 outbreak, combined with the age-dependent infection pattern observed before the recent outbreak in Manaus, suggests that OROV infection elicits a long-lived antibody response. We also found that OROV-specific IgM antibodies have a higher neutralizing capacity against OROV isolate, which aligns with findings from an experimental mouse study that demonstrated that IgM produced during primary infection is essential for controlling OROV replication and preventing neurological disease[33]. However, this higher IgM neutralizing capacity appears to be restricted to the contemporary OROV isolate, which is likely to be the OROV strain that caused these infections.

We estimated that between 1960 and 2025, OROV caused around 9.4 million infections across the Americas. Our findings indicate that the historical underreporting of OROV infections is probably owing to, at least in part, low surveillance capacity and limited healthcare access across countries in the Amazon Basin. The cumulative number of OROV infections reported is substantially lower than the estimated 5 million annual CHIKV infections in the Americas[34], a major arbovirus that causes explosive outbreaks. These differences in the number of infections for the two arboviral diseases appear linked to distinct transmission dynamics, primarily driven by vector ecology. OROV is probably mainly transmitted by *C. paraensis*, which is associated with high moisture levels and found predominantly in forest and rural areas[23,35]. For instance, our analysis indicates that wet season (December to May) in Amazonas state exhibits higher climate suitability for *C. paraensis*, which is consistent with data from entomological fieldwork that demonstrated that *C. paraensis* is predominantly abundant during the wet season, specifically when temperatures range between 30 °C and 32 °C and relative air humidity is between 75% and 85%, compared to the dry season in the Amazon region[36]. By contrast, CHIKV is transmitted by *Aedes aegypti* and, to some extent, by *Aedes albopictus*, both invasive anthropophilic mosquito species in urban centers[37]. Consequently, OROV appears to have a greater impact on rural communities, whereas CHIKV significantly affects overall public health owing to a larger number of cases occurring in densely populated urban areas. In addition, OROV infection is usually a mild febrile illness, which contrasts with the typically symptomatic and often debilitating disease caused by CHIKV infection[37,38]. For instance, while the rate of symptomatic CHIKV infections in the Americas is estimated at 51% (ref. 39), it is plausible that the proportion of asymptomatic or oligosymptomatic OROV infections is similar to that of Zika virus and West Nile virus, which is estimated to be around 80% (refs. 15,40). Future studies are needed to investigate the proportion of OROV asymptomatic cases.

https://doi.org/10.1038/s41591-026-04221-z

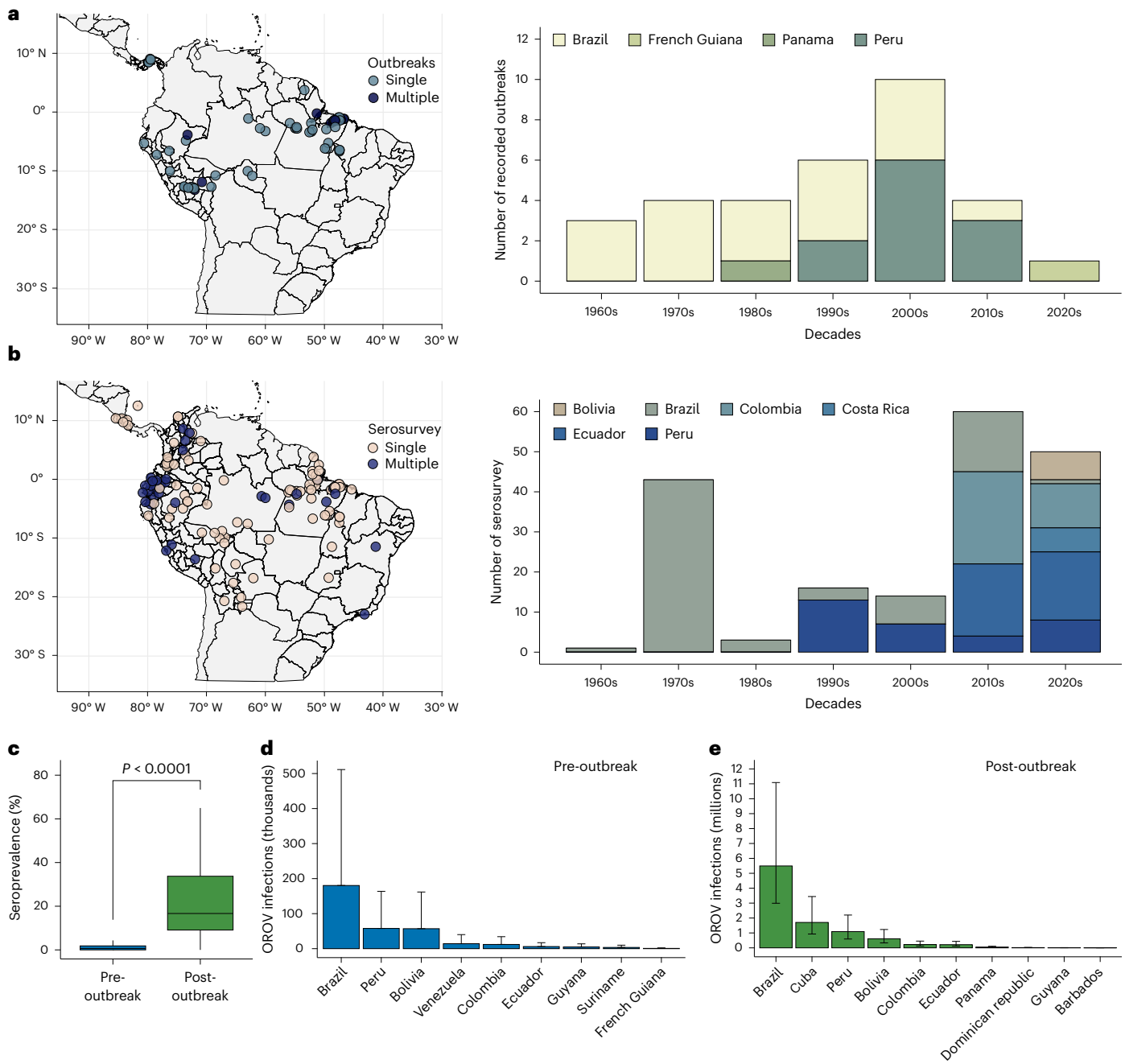

Fig. 5 | Estimated number of OROV infections in Latin America and the Caribbean. a, The spatiotemporal distribution of major OROV outbreaks documented in Latin America between 1961 and 2020 ($n = 32$). **b**, The spatiotemporal distribution of OROV seroprevalence studies conducted in Latin America and the Caribbean between 1961 and 2022 ($n = 187$). **c**, OROV seroprevalence in locations before ($n = 118$) and after documented outbreaks ($n = 69$). The box plots show the median (middle line), the 25th and 75th percentiles (box) and the lowest and highest values within 1.5× IQR from the first and third quartiles (whiskers). The P value ($P < 0.0001$) was calculated using the two-sided Wilcoxon rank sum test. **d**, The estimated number of OROV infections in administrative units (states, departments or provinces) located within the Amazon region across nine South American countries based on a scenario of continuous endemic transmission (that is, using seroprevalence data from before major outbreaks). The bar represents the median value and the error bars show the 75th percentile. **e**, The estimated number of cumulative OROV infections in administrative units that had reported Oropouche fever outbreaks in ten Latin American and Caribbean countries and territories based on a scenario including major outbreaks (that is, using seroprevalence data from after major outbreaks). The bar represents the median and the error bars show the 25th and 75th percentiles. Shapefile in **a** and **b** from the Instituto Brasileiro de Georgrafia e Estatística under a Creative Commons license CC BY 4.0 and Epi Info, US Centers for Disease Control and Prevention under a Creative Commons license CC0 1.0.

This study has several limitations. First, our seroprevalence data rely on convenience blood donor samples, which limits the generalization of our seroprevalence and demographic findings to the broader population. Second, OROV infections have probably been underestimated in past years owing to variable healthcare-seeking behaviors, absence of diagnostic capabilities and a limited OROV surveillance system in many endemic areas. These factors may have contributed to underreported incidence rates. In addition, further studies with structured analysis using country-level diagnosis proxies are necessary to determine underreporting of OROV infection cases. Third, our historical reconstruction is based on a serocatalytic model with assumptions that may oversimplify the complex, long-term dynamics of OROV

https://doi.org/10.1038/s41591-026-04221-z

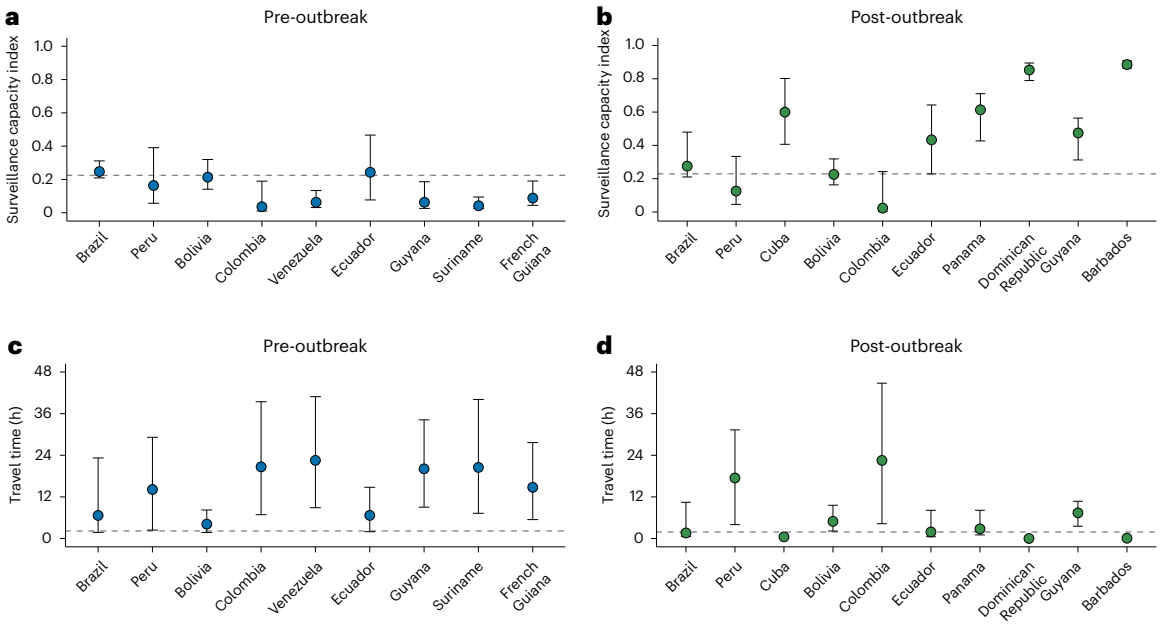

Fig. 6 | Surveillance capacity and healthcare accessibility in OROV-affected regions. a,**b**, The model-predicted relative surveillance capacity index for emerging acute viral infection diseases, focusing on historical endemic areas in the Amazon Basin collected pre-outbreak (**a**) and post-outbreak (**b**). Data are represented as medians (dots) with interquartile range (bars). The dashed line in **a** represents the median surveillance capacity in the South American continent (0.2246) and the dashed line in **b** represents the median surveillance capacity in Latin America and the Caribbean (0.2337). The index ranges from 0 (lowest) to 1 (highest), indicating surveillance capacity[41]. **c**,**d**, The optimal travel time in hours for individuals with access to motorized transportation (for example, car and motorcycle) to healthcare facilities (for example, hospital or clinic)[42], focusing on areas recently affected by the 2024–2025 epidemic collected pre-outbreak (**c**) and post-outbreak (**d**). Data are represented as medians (dots) with interquartile range (bars). The dashed line in **c** represents the median travel time to healthcare in South America (approximately 2 h and 10 min) and the dashed line in **d** represents the median travel time to healthcare in Latin America and the Caribbean (approximately 1 h and 53 min). Surveillance capacity and healthcare accessibility data were extracted at the state, department or province level for pre-outbreak and post-outbreak periods.

circulation. Finally, our estimate of OROV infections relied on available cross-sectional seroprevalence studies, which were conducted using varying protocols and assays. This heterogeneity in the data is also a strength due to multiple locations, years and laboratories. However, it may also be affected by the potential sensitivity and specificity of assays used, as well as false-positive results from other circulating orthobunyaviruses in these communities, which could affect the accuracy of our infection estimates.

In conclusion, our study provides important context about the dynamics and drivers of OROV transmission in Manaus during the early stage of the ongoing epidemic in South and Central America. We showed that historical OROV transmission in the Amazon region has been characterized by infrequent, short and limited outbreaks; however, the long-term impact of the OROV epidemic in newly affected areas after 2024 remains to be further investigated. We also estimated the cumulative number of OROV infections in Latin America and the Caribbean. This information may help inform future studies and public health strategies aimed at mitigating the effects of OROV outbreaks and epidemics.

Online content

Any methods, additional references, Nature Portfolio reporting summaries, source data, extended data, supplementary information, acknowledgements, peer review information; details of author contributions and competing interests; and statements of data and code availability are available at https://doi.org/10.1038/s41591-026-04221-z.

References

1. Travassos da Rosa, J. F. et al. Oropouche virus: clinical, epidemiological, and molecular aspects of a neglected orthobunyavirus. *Am. J. Trop. Med. Hyg.* **96**, 1019–1030 (2017).
2. de Souza, W. M. et al. ICTV virus taxonomy profile: *Peribunyaviridae* 2024. *J. Gen. Virol.* https://doi.org/10.1099/jgv.0.002034 (2024).
3. de Lima, S. T. S. et al. Molecular epidemiology of Oropouche virus, Ceará State, Brazil, 2024. *Emerg. Infect. Dis.* **31**, 838–842 (2025).
4. das Neves Martins, F. E. et al. Newborns with microcephaly in Brazil and potential vertical transmission of Oropouche virus: a case series. *Lancet Infect. Dis.* **25**, 155–165 (2025).
5. Bandeira, A. C. et al. Fatal Oropouche virus infections in nonendemic region, Brazil, 2024. *Emerg. Infect. Dis.* **30**, 2370–2374 (2024).
6. Hughes, H. R. et al. ICTV virus taxonomy profile: *Peribunyaviridae*. *J. Gen. Virol.* **101**, 1–2 (2020).
7. Tilston-Lunel, N. L. Oropouche virus: an emerging orthobunyavirus. *J. Gen. Virol.* **105**, 002027 (2024).
8. Aguilar, P. V. et al. Iquitos virus: a novel reassortant Orthobunyavirus associated with human illness in Peru. *PLoS Negl. Trop. Dis.* **5**, e1315 (2011).
9. Ladner, J. T. et al. Genomic and phylogenetic characterization of viruses included in the Manzanilla and Oropouche species complexes of the genus *Orthobunyavirus*, family *Bunyaviridae*. *J. Gen. Virol.* **95**, 1055–1066 (2014).
10. Tilston-Lunel, N. L. et al. Genetic analysis of members of the species Oropouche virus and identification of a novel M segment sequence. *J. Gen. Virol.* **96**, 1636–1650 (2015).
11. Briese, T., Bird, B., Kapoor, V., Nichol, S. T. & Lipkin, W. I. Batai and Ngari viruses: M segment reassortment and association with severe febrile disease outbreaks in East Africa. *J. Virol.* **80**, 5627–5630 (2006).
12. Scachetti, G. C. et al. Re-emergence of Oropouche virus between 2023 and 2024 in Brazil: an observational epidemiological study. *Lancet Infect. Dis.* **25**, 166–175 (2025).

13. Naveca, F. G. et al. Human outbreaks of a novel reassortant Oropouche virus in the Brazilian Amazon region. *Nat. Med.* **30**, 3509–3521 (2024).
14. Srivastava, S. et al. The emergence of oropouche fever: a potential new threat? *New Microbes New Infect.* **65**, 101596 (2025).
15. McDonald, E. et al. Surveillance for West Nile virus disease—United States, 2009–2018. *Am. J. Transplant.* **21**, 1959–1974 (2021).
16. Rodriguez-Morales, A. J. et al. Reemergence of Oropouche virus infection in Ecuador, 2024: vectors and cases. *J. Infect.* **91**, 106544 (2025).
17. Bello-Rodríguez, B. M., Vega-Jiménez, J., Cañete, R. & Rodriguez-Morales, A. J. Emergence of Oropouche virus infection in Matanzas, Cuba, 2024. *J. Infect.* **90**, 106470 (2025).
18. Cruz, C. D. et al. Co-circulation of 2 Oropouche virus lineages during outbreak, Amazon region of Peru, 2023–2024. *Emerg. Infect. Dis.* **31**, 879–881 (2025).
19. Usuga, J. et al. Co-circulation of 2 Oropouche virus lineages, Amazon Basin, Colombia, 2024. *Emerg. Infect. Dis.* **30**, 2375–2380 (2024).
20. Capobianchi, M. R., Castilletti, C. & Gobbi, F. G. Potential risks of Oropouche virus importation into Europe. *J. Travel Med.* **31**, taae109 (2024).
21. Morrison, A. et al. Oropouche virus disease among US travelers—United States, 2024. *MMWR Morb. Mortal. Wkly Rep.* **73**, 769–773 (2024).
22. Scroggs, S. L. P. et al. Enhanced infection and transmission of the 2022–2024 Oropouche virus strain in the North American biting midge *Culicoides sonorensis*. *Sci. Rep.* **15**, 27368 (2025).
23. Gräf, T. et al. Expansion of Oropouche virus in non-endemic Brazilian regions: analysis of genomic characterisation and ecological drivers. *Lancet Infect. Dis.* **25**, 379–389 (2025).
24. Lapola, D. M. et al. The drivers and impacts of Amazon forest degradation. *Science* **379**, eabp8622 (2023).
25. Borborema, C. A. et al. [1st occurrence of outbreaks caused by Oropouche virus in the State of Amazonas]. *Rev. Inst. Med. Trop. Sao Paulo* **24**, 132–139 (1982).
26. Fischer, C. et al. The spatiotemporal ecology of Oropouche virus across Latin America: a multidisciplinary, laboratory-based, modelling study. *Lancet Infect. Dis.* **25**, 1020–1032 (2025).
27. de Melo Iani, F. C. et al. Travel-associated international spread of Oropouche virus beyond the Amazon. *J. Travel Med.* **32**, taaf018 (2025).
28. Tian, H. et al. Increasing airline travel may facilitate co-circulation of multiple dengue virus serotypes in Asia. *PLoS Negl. Trop. Dis.* **11**, e0005694 (2017).
29. Nunes, M. R. et al. Air travel is associated with intracontinental spread of dengue virus serotypes 1–3 in Brazil. *PLoS Negl. Trop. Dis.* **8**, e2769 (2014).
30. Nunes, M. R. et al. Emergence and potential for spread of Chikungunya virus in Brazil. *BMC Med.* **13**, 102 (2015).
31. Faria, N. R. et al. Zika virus in the Americas: early epidemiological and genetic findings. *Science* **352**, 345–349 (2016).
32. de Souza, W. M. & Weaver, S. C. Effects of climate change and human activities on vector-borne diseases. *Nat. Rev. Microbiol.* **22**, 476–491 (2024).
33. Toledo-Teixeira, D. A. et al. MyD88 signalling in B cells and antibody responses during Oropouche virus-induced neurological disease in mice. *eBioMedicine* **117**, 105815 (2025).
34. Ribeiro Dos Santos, G. et al. Global burden of chikungunya virus infections and the potential benefit of vaccination campaigns. *Nat. Med.* **31**, 2342–2349 (2025).
35. Mellor, P. S., Boorman, J. & Baylis, M. Culicoides biting midges: their role as arbovirus vectors. *Annu. Rev. Entomol.* **45**, 307–340 (2000).
36. Feitoza, L. H. M. et al. Influence of meteorological and seasonal parameters on the activity of *Culicoides paraensis* (Diptera: *Ceratopogonidae*), an annoying anthropophilic biting midge and putative vector of Oropouche Virus in Rondônia, Brazilian Amazon. *Acta Trop.* **243**, 106928 (2023).
37. de Souza, W. M., Lecuit, M. & Weaver, S. C. Chikungunya virus and other emerging arthritogenic alphaviruses. *Nat. Rev. Microbiol.* **23**, 585–601 (2025).
38. de Souza, W. M. et al. Chikungunya: a decade of burden in the Americas. *Lancet Reg. Health Am.* **30**, 100673 (2024).
39. Bustos Carrillo, F. et al. Epidemiological evidence for lineage-specific differences in the risk of inapparent Chikungunya virus infection. *J. Virol.* https://doi.org/10.1128/JVI.01622-18 (2019).
40. Duffy, M. R. et al. Zika virus outbreak on Yap Island, Federated States of Micronesia. *N. Engl. J. Med.* **360**, 2536–2543 (2009).
41. Lim, A. et al. The overlapping global distribution of dengue, Chikungunya, Zika and yellow fever. *Nat. Commun.* **16**, 3418 (2025).
42. Weiss, D. J. et al. Global maps of travel time to healthcare facilities. *Nat. Med.* **26**, 1835–1838 (2020).

Erika R. Manuli[1,2,3,19], Xinyi Hua[4,19], Gabriel C. Scachetti[5,19], Julia Forato[4,5,19], Ingra M. Claro[4], Geovana M. Pereira[2], Livia Sacchetto[5], Oscar Cortes-Azuero[6], Ana Carolina Bernardo[7], Cláudia F. Resende[7], Natália B. S. Bacarov[7], Ligia Capuani[2], Shirlene T. S. de Lima[4,5], Ronaldo de Jesus[8], Rodrigo B. Kato[8], Bárbara B. Salgado[9], Carolina M. L. Singh[9], Nadielle C. Pereira[9], Renato S. Reis[10], Sérgio R. L. Albuquerque[11], Richard Stanton[12], Vanderson S. Sampaio[13], Ana I. Bento[14], Marielton P. Cunha[5], Oliver Ratmann[15], Nuno R. Faria[2,16], Scott C. Weaver[17], Pritesh J. Lalwani[9], Henrik Salje[6], Allyson G. Costa[11], José Luiz Proenca-Modena[5,20] ✉, Ester C. Sabino[1,18,20] ✉ & William M. de Souza[4,20] ✉

[1]Programa de Pós-Graduação em Doenças Infecciosas e Saúde Global, Departamento de Infectologia e Medicina Tropical, Faculdade de Medicina, Universidade de São Paulo, São Paulo, Brazil. [2]Instituto de Medicina Tropical, Faculdade de Medicina, Universidade de São Paulo, São Paulo, Brazil. [3]Departamento de Pesquisa Clínica e Inovação em Saúde, Universidade Municipal de São Caetano do Sul, São Paulo, Brazil. [4]Department of Microbiology, Immunology, and Molecular Genetics, College of Medicine, University of Kentucky, Lexington, KY, USA. [5]Department of Genetics, Microbiology and Immunology, Institute of Biology, University of Campinas, Campinas, Brazil. [6]Department of Genetics, University of Cambridge, Cambridge, UK. [7]EUROInstitute, EUROIMMUN Brasil, São Caetano do Sul, Brazil. [8]Instituto de Ciências Biológicas, Universidade Federal de Minas Gerais,

Belo Horizonte, Brazil. [9]Instituto Leônidas e Maria Deane, Fiocruz Amazônia, Manaus, Brazil. [10]Instituto de Saúde e Biotecnologia, Universidade Federal do Amazonas, Coari, Brazil. [11]Instituto de Ciências Biológicas, Universidade Federal do Amazonas, Manaus, Brazil e Diretoria de Ensino e Pesquisa, Fundação Hospitalar de Hematologia e Hemoterapia do Amazonas, Manaus, Brazil. [12]Division of Infection and Immunity, Cardiff University School of Medicine, University Hospital of Wales, Cardiff, UK. [13]Instituto Todos Pela Saúde, São Paulo, Brazil. [14]Department of Public and Ecosystem Health, College of Veterinary Medicine, Cornell University, Ithaca, NY, USA. [15]Department of Mathematics, Imperial College London, London, UK. [16]MRC Centre for Global Infectious Disease Analysis, Department of Infectious Disease Epidemiology, School of Public Health, Imperial College London, London, UK. [17]Department of Microbiology and Immunology, University of Texas Medical Branch, Galveston, TX, USA. [18]Departamento de Patologia, Faculdade de Medicina, Universidade de São Paulo, São Paulo, Brazil. [19]These authors contributed equally: Erika R. Manuli, Xinyi Hua, Gabriel C. Scachetti, Julia Forato [20]These authors jointly supervised this work: José Luiz Proenca-Modena, Ester C. Sabino, William M. de Souza. ✉e-mail: jlmodena@unicamp.br; sabinoec@usp.br; wmdesouza@uky.edu

Methods

Serosurvey design and population

We retrospectively tested anonymized serum samples from two distinct cohorts of Manaus residents. We did not perform a formal sample size calculation for either cohort. The first cohort comprised residual blood samples from Hemoterapia do Amazonas. We retrieved stored residual laboratory screening samples from routine blood donors in November 2023, June 2024 and November 2024. We selected 2,055 samples (685 ×3 time points) from blood donors to geographically represent Manaus by using the ZIP codes of blood donors. The second cohort consisted of blood samples collected from Manaus residents (general population, $n = 440$ participants) between 2015 and 2016, at which time no participants reported any symptoms. All donors with recorded age and sex were eligible for testing, both self-reported and only age variables were analyzed. No participant compensation was provided in this study. The ethics committee waived the requirement for informed consent for the use of residual blood bank samples (2023–2024). For the second cohort (2015–2016), written informed consent was obtained from all adult participants and permission for minors was provided by their legally authorized representatives. Upon arrival at the laboratory, blood samples from both cohorts were centrifuged at 1,000*g* for 15 min to separate the serum, which was then stored at −80 °C.

Inclusion and ethics statement

This study is the result of an equitable international collaboration among research teams from Brazil, the USA and the UK. Our teams have been contributing to understanding transmission dynamics and virus–host interactions of arboviruses that cause diseases in humans, combining genomics, data science and experimental virology to understand, prevent and mitigate arboviral diseases. This research was primarily conducted and led by Brazilian researchers, with contributions from international researchers in serocatalytic modeling and epidemiology. All international partners invited to collaborate with this study have a longstanding history dedicated to strengthening local infrastructure, disseminating data and sharing resources throughout Latin America and the Caribbean. Furthermore, we are committed to training, supporting and fostering the success of local scientists across Latin America and the Caribbean by promoting ethical research practices to reduce inequities.

Ethics approval

All procedures were conducted with the approval of the Ethics Committees of the University of São Paulo (approval number 73030523.6.1001.0068) and the Federal University of Amazonas (approval numbers 5.876.612 and 6.629.451).

Oropouche fever laboratory-confirmed cases

We use individualized and de-identified clinical data on Oropouche fever cases from Brazil. National epidemiological data of laboratory-confirmed cases were obtained from the Brazilian Ministry of Health. This dataset includes patient-level information on age, sex, state and municipality residence, date of sample collection and diagnosis method collected from 1 January 2014 to 31 December 2024. Sex data were obtained through self-reporting, offering options for sex as male or female. All cases included in this study were laboratory-confirmed cases defined as a suspected patient with one positive laboratory result for OROV, either by reverse-transcription quantitative polymerase chain reaction, immunoglobulin M (IgM) detection and/or viral isolation (Vero and C6/36 cells). No cases defined by only clinical epidemiological criteria were included in this study.

Incidence and age–sex distribution

Incidence rates and age–sex distribution were calculated using Brazilian national epidemiological data of laboratory-confirmed cases and population data from the 2010 and 2022 Brazilian censuses, as reported by the Brazilian Institute of Geography and Statistics[43,44]. Annual testing positivity rates were determined by dividing the number of laboratory-confirmed cases by the total number of patients tested for OROV at Manaus, Amazonas and Brazil. The 95% CIs were calculated using the Clopper–Pearson exact method.

Oropouche transmission suitability index

We estimated the climate suitability for OROV transmission using a previously published Index P measure[45]. Index P estimates the arboviral transmission potential based on daily temperature and relative humidity data within a mechanistic climate-driven transmission model, which employs a Bayesian Markov Chain Monte Carlo framework[45]. The model incorporates daily temperature and relative humidity data, along with seven normal prior distributions (each defined by a distinct mean and standard deviation) of entomological and host parameters. In brief, we obtained daily 2-m temperature and 2-m dewpoint temperature between 1 January 2014 and 31 December 2024, from the fifth generation of the European Centre for Medium-Range Weather Forecasts global atmospheric reanalysis datasets[46]. We combined these data with ecological and entomological priors for *C. paraensis* documented in the literature[35,47–51] (Extended Data Table 1). Next, we use the R package MVSE[45] to estimate daily transmission potential (Index P) for each month from 2014 to 2024, aggregating it to a single mean value per calendar month for all municipalities in Amazonas state ($n = 62$). We also calculated the mean Index P for the wet (December to May) and dry (June to November) seasons by averaging the monthly values for each season across 62 municipalities in Amazonas state. Then, we combined the mean Index P value for each calendar month and for the wet and dry seasons with the municipality-level shapefile of Amazonas state to generate the index P maps using the R package.

OROV-specific antibodies IgG and IgM detection ELISA

We used a commercial ELISA from Euroimmun Medizinische Diagnostika AG to detect OROV-specific IgG (EI 2771-9601 G) and IgM (EI 2771-9601 M). Serum samples were analyzed at a 1:100 dilution using the automated EUROIMMUN Analyzer I. For IgG, we defined a sample as positive if ≥22 RU ml^{-1}, negative if <16 RU ml^{-1} and borderline if the range was ≥16 to <22 RU ml^{-1} following the instructions of the manufacturers. For IgM, a sample was defined as positive if the ratio was ≥1.1, negative if <0.8 and borderline if the ratio was between ≥0.8 and <1.1. We conducted the two-sided Wilcoxon rank sum test to compare OROV-specific IgG concentration (RU ml^{-1}) determined by ELISA in serum samples from individuals aged <50 years and ≥50 years collected pre-outbreak and post-outbreak. This nonparametric test was used because observations were independent and the normality of the data was not assumed.

FRNT for OROV

A FRNT was performed to detect the neutralizing antibodies against OROV in human serum samples, as previously described[12]. Briefly, samples were heat inactivated at 56 °C per 15 min, then diluted 1:10 in Dulbecco's modified Eagle medium (DMEM) and incubated for 1 h at 37 °C with 2×10^3 PFU ml^{-1} of OROV AM0088 isolate. Next, 100 µl of the virus–serum mixtures were added to 96-well plates containing Vero CCL-81 cells (ATTC) with 5×10^4 cells per well at 80% confluence and incubated for 1 h at 37 °C with 5% CO_2 for viral adsorption. Subsequently, 125 µl of DMEM with 0.75% carboxymethylcellulose and 5% fetal bovine serum (FBS) were added to the wells and plates were incubated at 37 °C with 5% CO_2 for 48 h. Cells were then fixed with 70 µl of 8% paraformaldehyde for 1 h at 4 °C. After removing the paraformaldehyde, cells were washed with phosphate-buffered saline (PBS) and blocked for 30 min with 150 µl of blotto. Following blocking, monolayers were washed with Perm/Wash Buffer (PBS with 0.1% bovine serum albumin and 0.1% Triton X-100) and incubated with a polyclonal anti-OROV

antibody (VR-1228AF, ATTC) at a dilution of 1:1,000. After a second wash, an anti-mouse IgG secondary antibody (AP124P, Sigma-Aldrich) at a dilution 2:1,000 was added. The assay was revealed with True-Blue Peroxidase substrate (5510-0030, KPL) for 30 min after a final wash. OROV neutralizing serum samples were defined as those that promoted at least a 50% reduction in focus formation compared to the positive control. Cell lines were free of mycoplasma, confirmed by periodic testing for contamination using the LookOut Mycoplasma PCR Detection kit (MP0035-1KT, Sigma-Aldrich).

Plaque reduction neutralization test for OROV

To compare the neutralizing antibody capacity of serum from previously infected individuals against OROV strains BeAn19991 (1960, prototype) and AM0088 (2024, reassortment), we performed a $PRNT_{50}$ as previously described[12,52]. Serum samples were heat inactivated at 56 °C per 15 min to inactivate the complement system. We then performed serial dilutions and incubated each sample for 1 h at 37 °C with a solution containing either 2×10^3 PFU ml^{-1} of the BeAn19991 isolate or 80 PFU ml^{-1} of the AM0088 isolate. The virus–serum mixtures were added to preformed Vero CCL-81 cell monolayers and incubated for 1 h at 37 °C with 5% CO_2 for viral adsorption. After removing the inoculum, 1 ml of DMEM containing 0.75% carboxymethylcellulose and 5% FBS was added to each well and the plates were incubated for 3 days under the same conditions. The cells were then fixed with 500 µl of 8% paraformaldehyde for 1 h and stained with 1% methylene blue for 5 min. Plaque reduction was calculated as the percentage of plaques counted compared to the positive control, based on the average of two technical duplicates. These values were then transformed to $\log_{10}$ and subjected to a three-parameter nonlinear dose–response inhibition regression test.

Comparison between ELISA and FNRT and ELISA binding antibodies

To assess the agreement between the two anti-OROV IgG assays (EUROIMMUN and FRNT), we calculated the percentage of concordance by dividing the total number of samples that tested positive or negative in both assays by the total number of samples tested. The Wilcoxon rank-sum test was used to compare the distributions of OROV-specific IgG concentration (RU ml^{-1}) between the two age groups. The same test was also employed to compare OROV seroprevalence distributions in locations before and after documented outbreaks.

Seroprevalence and reconstruction from previous OROV outbreaks

We calculated the observed seroprevalence for each serosurvey by dividing the number of positive cases by the total number of samples tested. The 95% CIs were calculated using the Clopper–Pearson exact method. Next, we prepared individual seroepidemiological data (age, serostatus and year of serosurvey) from four serosurveys (2015–2016, November 2023, June 2024 and November 2024) to fit multiple serocatalytic models (that is, constant, piecewise, outbreak, constant transmission with outbreak and independent) using the R package Rsero[53]. Based on model performance metrics and inspection, we identified the constant transmission with one outbreak model as the best fit for all four serosurveys. From the model's posterior distribution, we then extracted the median and 95% credible intervals for the probable outbreak years and attack rates.

Major OROV outbreaks

To identify major OROV outbreaks, we conducted a systematic search of published literature and reports. Our search included PubMed (search term 'Oropouche' AND 'outbreak'), Pan American Health Organization (PAHO) website (search term 'Oropouche'), ProMED (search term 'Oropouche') and Google (search term 'Oropouche' AND 'outbreak') without language restriction. We also consulted the Ministry of Health websites when possible. For each country and territory, we search for evidence of a major OROV outbreak, defined as a case series of Oropouche fever. Evidence included detection of OROV via viral isolation, PCR, IgM or seroprevalence studies (IgG or IgM) with a documented period of increased cases. We considered outbreaks that occurred between 1960 and 2022, excluding single case reports. For each identified outbreak, we recorded the location (municipality, state and national level), year and duration in months[7,25,54–77] (Extended Data Table 4). Outbreaks that affected neighboring municipalities or states and overlapped in time were considered to be a single event. The spatiotemporal distribution of major OROV outbreaks was presented in a map and time series using the R package.

OROV serosurveys

To compile seroepidemiological data, we conducted a systematic search of published literature in PubMed and Google using the terms 'Oropouche', 'serosurvey', 'epidemiology' and 'antibodies' with no language restrictions. We defined a serosurvey site as a study conducted within a distinct municipality in a specific year. If a municipality was studied in multiple years, each instance was considered an independent seroepidemiological study. For each study, we recorded the location (national and state level), number of positive samples, total samples tested, positive rate, age range, assay type (for example, ELISA, PRNT and hemagglutination inhibition assay) and assay target (IgM and IgG antibodies). We also categorized each serosurvey as either before or after a documented major OROV outbreak[8,25,26,54,55,57,58,60,61,63,66,67,76,78–91] (Supplementary Table 1). The spatiotemporal distribution of these major outbreaks was then presented in a map and time series using the R package. For serosurveys with an undetermined municipality, we displayed the location at the centroid of the corresponding state.

Estimate the number of OROV infections

To estimate the number of OROV infections, we used the median and interquartile range (25th and 75th percentiles) from seroprevalence studies. We conducted this estimation under two scenarios: first, for the continuous endemic OROV transmission scenario, we focused on the Amazon Basin (historical OROV endemic areas) across Brazil, Peru, Colombia, Bolivia, Ecuador, French Guiana, Guyana, Suriname and Venezuela. We used the pre-outbreak seroprevalence range for these locations, specifically the median and interquartile range. We excluded the 25th percentile for this estimate because its value was calculated as 0, indicating nontransmission. Second, for a major OROV outbreak scenario, we considered all locations identified with major OROV outbreaks between 1960 and 2022, as well as locations with documented autochthonous OROV outbreaks during the 2024–2025 epidemic in Latin America and the Caribbean. These were identified from PAHO reports and published articles, and we used state-level case series owing to a lack of available data at the municipal level. The estimates were determined based on the median and interquartile range of seroprevalence from post-outbreak sites in our literature review. For population data, we used the municipality level for outbreaks in Brazil with an incidence of at least 1 (that is, 1 case per 100,000 inhabitants). For other countries, we obtained the state-level population data from their respective national censuses. We conducted the two-sided Wilcoxon rank sum test to compare seroprevalence between the two scenarios. This nonparametric test was used because observations were independent and the normality of the data was not assumed.

Surveillance capacity and optimal travel time to healthcare facilities

To examine the surveillance capacity and healthcare accessibility in OROV endemic areas, we utilized raster files with model-predicted relative surveillance capability for emerging acute viral infectious disease optimal travel time to healthcare facilities via motorized transport, as described elsewhere[41,42]. Next, we obtained shapefiles for the studied

areas from the Global Administrative Areas Database[92] and the R package rnaturalearth[93]. We then harmonized the geographic coordinate reference system and projected the surveillance and travel time raster files onto continental, national and subadministrative units (for example, states/provinces). Finally, we extracted the median, 25th and 75th percentiles for each of the described locations.

Statistics and reproducibility

Sample sizes were not predetermined by statistical power calculations. Of the 440 total samples collected during the 2015–2016 serosurvey, 126 were excluded (115 seronegative and 11 seropositive) owing to missing birth dates or age at the time of collection. These exclusions were necessary for the implementation of the age-structured serocatalytic models (Fig. 4b,c). No other data were excluded from the analyses. A two-sided Wilcoxon rank-sum test was used to compare OROV-specific IgG concentrations (RU ml^{-1}) between age groups (<50 versus ≥50 years) across pre- and post-outbreak serum samples (Fig. 3c). This same approach was applied to assess differences in OROV seroprevalence across locations before and after documented outbreaks (Fig. 5c).

Reporting summary

Further information on research design is available in the Nature Portfolio Reporting Summary linked to this article.

Data availability

All codes and data used to generate the figures in this article are publicly available via GitHub at https://github.com/wmarciel/Oropouche-LAC. We obtained shapefiles from the Brazilian Institute of Geography and Statistics and the Centers for Disease Control and Prevention, respectively. De-identified individual-level data from the Brazilian Ministry of Health can be provided for research purposes after approval by a committee on human experimentation (if applicable). These data can be obtained upon request to the corresponding authors. The estimated response time from the corresponding authors may be up to 3 weeks.

References

43. Population Census 2022. *Instituto Brasileiro de Geografia e Estatística* https://www.ibge.gov.br/en/statistics/social/labor/22836-2022-census-3.html (2022).
44. Population Census 2010. *Instituto Brasileiro de Geografia e Estatística* https://www.ibge.gov.br/en/statistics/social/labor/18391-2010-population-census.html?edicao=19720 (2010).
45. Obolski, U. et al. MVSE: an R-package that estimates a climate-driven mosquito-borne viral suitability index. *Methods Ecol. Evol.* **10**, 1357–1370 (2019).
46. ERA5 hourly data on single levels from 1940 to present. *Climate Data Store* https://cds.climate.copernicus.eu/datasets/reanalysis-era5-single-levels?tab=overview (2025).
47. Pinheiro, F. P., Hoch, A. L., Gomes, M. L. & Roberts, D. R. Oropouche virus. IV. Laboratory transmission by *Culicoides paraensis*. *Am. J. Trop. Med. Hyg.* **30**, 172–176 (1981).
48. Mercer, D. R., Spinelli, G. R., Watts, D. M. & Tesh, R. B. Biting rates and developmental substrates for biting midges (Diptera: *Ceratopogonidae*) in Iquitos, Peru. *J. Med. Entomol.* **40**, 807–812 (2003).
49. In 2023, life expectancy reaches 76.4 years; surpasses pre-pandemic level. *Instituto Brasileiro de Geografia e Estatística* https://agenciadenoticias.ibge.gov.br/en/agencia-news/2184-news-agency/news/42021-in-2023-life-expectancy-reaches-76-4-years-surpasses-pre-pandemic-level (2024).
50. Guagliardo, S. A. J. et al. Estimation of incubation period for Oropouche virus disease among travel-associated cases, 2024–2025. *Emerg. Infect. Dis.* **31**, 1337–1343 (2025).
51. Pinheiro, F. P., Travassos da Rosa, A. P., Gomes, M. L., LeDuc, J. W. & Hoch, A. L. Transmission of Oropouche virus from man to hamster by the midge *Culicoides paraensis*. *Science* **215**, 1251–1253 (1982).
52. Proenca-Modena, J. L. et al. Interferon-regulatory factor 5-dependent signaling restricts Orthobunyavirus dissemination to the central nervous system. *J. Virol.* **90**, 189–205 (2016).
53. Hoze, N. et al. RSero: a user-friendly R package to reconstruct pathogen circulation history from seroprevalence studies. *PLoS Comput. Biol.* **21**, e1012777 (2025).
54. Pinheiro, F. P. et al. Oropouche virus. I. A review of clinical, epidemiological, and ecological findings. *Am. J. Trop. Med. Hyg.* **30**, 149–160 (1981).
55. Pinheiro, F. F., Pinheiro, M., Bensabath, G., Caucsey, O. R. & Shope, R. Epidemia de vírus Oropouche em Belém. *Mem. Inst. Evandro Chagas* **12**, 15–23 (1962).
56. Pinheiro, F. P., Travassos da Rosa, A. P. A. & Vasconcelos, P. F. C. in *An Overview of Arbovirology in Brazil and Neighbouring Countries* (eds Travassos da Rosa, A. P. A. et al.) 186–192 (Instituto Evandro Chagas, 1998).
57. Pinheiro, F. P., Travassos da Rosa, A. P., Travassos da Rosa, J. F. & Bensabath, G. An outbreak of Oropouche virus diease in the vicinity of Santarem, Para, Brazil. *Tropenmed. Parasitol.* **27**, 213–223 (1976).
58. LeDuc, J. W., Hoch, A. L., Pinheiro, F. P. & da Rosa, A. P. Epidemic Oropouche virus disease in northern Brazil. *Bull. Pan Am. Health Organ.* **15**, 97–103 (1981).
59. Tesh, R. B. The emerging epidemiology of Venezuelan hemorrhagic fever and Oropouche fever in tropical South America. *Ann. N. Y. Acad. Sci.* **740**, 129–137 (1994).
60. Freitas, R. B. et al. in *Internacional Simposium on Tropical Arboviruses and Haemorrhagic Fevers* Vol. 25, 59–72 (Fundação Serviços de Saúde Pública, 1980).
61. Vasconcelos, P. F. et al. [1st register of an epidemic caused by Oropouche virus in the states of Maranhao and Goias, Brazil]. *Rev. Inst. Med. Trop. Sao Paulo* **31**, 271–278 (1989).
62. Vasconcelos, P. F. et al. Inadequate management of natural ecosystem in the Brazilian Amazon region results in the emergence and reemergence of arboviruses. *Cad. Saude Publica* **17**, 155–164 (2001).
63. Rosa, A. P. et al. [Outbreak of oropouche virus fever in Serra Pelada, municipality of Curionopolis, Para, 1994]. *Rev. Soc. Bras. Med. Trop.* **29**, 537–541 (1996).
64. Chavez, R., Colan, E. & Phillips, I. Fiebre de Oropouche en Iquitos: reporte preliminar de 5 casos. *Rev. Farmacol. Terap.* **2**, 12–14 (1992).
65. Forshey, B. M. et al. Arboviral etiologies of acute febrile illnesses in Western South America, 2000–2007. *PLoS Negl. Trop. Dis.* **4**, e787 (2010).
66. Azevedo, R. S. et al. Reemergence of Oropouche fever, northern Brazil. *Emerg. Infect. Dis.* **13**, 912–915 (2007).
67. Vasconcelos, H. B. et al. Oropouche fever epidemic in Northern Brazil: epidemiology and molecular characterization of isolates. *J. Clin. Virol.* **44**, 129–133 (2009).
68. Vasconcelos, H. B. et al. Molecular epidemiology of Oropouche virus, Brazil. *Emerg. Infect. Dis.* **17**, 800–806 (2011).
69. Alert ID: 449016 PRO/EDR Oropouche—Peru (02): (SM). *ProMED International Society for Infectious Diseases* www.promedmail.org (2010).
70. Alvarez-Falconi, P. P. & Rios Ruiz, B. A. Brote de fiebre de Oropuche en Bagazán, San Martín - Perú: evaluación epidemiológica, manifestaciones gastrointestinales y hemorrágicas. *Rev. Gastroenterol. Peru* **30**, 334–340 (2010).
71. Castro, S. et al. Brote de fiebre de Oropuche en dos localidades de la región Cajamarca, Perú, 2011. *Rev. Peru Epidemiol.* **17**, 1–6 (2013).

72. Romero-Alvarez, D. & Escobar, L. E. Vegetation loss and the 2016 Oropouche fever outbreak in Peru. *Mem. Inst. Oswaldo Cruz* **112**, 292–298 (2017).
73. Silva-Caso, W. et al. First outbreak of Oropouche Fever reported in a non-endemic western region of the Peruvian Amazon: molecular diagnosis and clinical characteristics. *Int. J. Infect. Dis.* **83**, 139–144 (2019).
74. Garcia, M. P. et al. [Detection of Oropouche viral circulation in Madre de Dios region, Peru (December 2015 to january 2016)]. *Rev. Peru. Med. Exp. Salud Publica* **33**, 380–381 (2016).
75. Martins-Luna, J. et al. Oropouche infection a neglected arbovirus in patients with acute febrile illness from the Peruvian coast. *BMC Res. Notes* **13**, 67 (2020).
76. Carvalho, V. L. et al. Arbovirus outbreak in a rural region of the Brazilian Amazon. *J. Clin. Virol.* **150-151**, 105155 (2022).
77. Gaillet, M. et al. Outbreak of Oropouche virus in French Guiana. *Emerg. Infect. Dis.* **27**, 2711–2714 (2021).
78. Dixon, K. E., Travassos da Rosa, A. P., Travassos da Rosa, J. F. & Llewellyn, C. H. Oropouche virus. II. Epidemiological observations during an epidemic in Santarem, Para, Brazil in 1975. *Am. J. Trop. Med. Hyg.* **30**, 161–164 (1981).
79. Watts, D. M. et al. Oropouche virus transmission in the Amazon River basin of Peru. *Am. J. Trop. Med. Hyg.* **56**, 148–152 (1997).
80. Watts, D. M. et al. Venezuelan equine encephalitis and Oropouche virus infections among Peruvian army troops in the Amazon region of Peru. *Am. J. Trop. Med. Hyg.* **56**, 661–667 (1997).
81. Baisley, K. J., Watts, D. M., Munstermann, L. E. & Wilson, M. L. Epidemiology of endemic Oropouche virus transmission in upper Amazonian Peru. *Am. J. Trop. Med. Hyg.* **59**, 710–716 (1998).
82. Tavares-Neto, J. et al. [Serologic survey for yellow fever and other arboviruses among inhabitants of Rio Branco, Brazil, before and three months after receiving the yellow fever 17D vaccine]. *Rev. Soc. Bras. Med. Trop.* **37**, 1–6 (2004).
83. Watts, D. M. et al. Etiologies of acute undifferentiated febrile illnesses in and near Iquitos from 1993 to 1999 in the Amazon River basin of Peru. *Am. J. Trop. Med. Hyg.* **107**, 1114–1128 (2022).
84. De Figueiredo, R. M. et al. [Exanthematous diseases and the first epidemic of dengue to occur in Manaus, Amazonas State, Brazil, during 1998–1999]. *Rev. Soc. Bras. Med. Trop.* **37**, 476–479 (2004).
85. Nunes, M. R. et al. Arbovirus eco-epidemiology in the area affected by the Cuiabá–Santarém Highway (BR-163), Pará State, Brazil]. *Cad. Saude Publica* **25**, 2583–2602 (2009).
86. Cruz, A. C. et al. [Serological survey for arboviruses in Juruti, Pará State, Brazil]. *Cad. Saude Publica* **25**, 2517–2523 (2009).
87. da Costa, V. G., de Rezende Feres, V. C., Saivish, M. V., de Lima Gimaque, J. B. & Moreli, M. L. Silent emergence of Mayaro and Oropouche viruses in humans in Central Brazil. *Int. J. Infect. Dis.* **62**, 84–85 (2017).
88. de Lima, R. C. et al. Oropouche virus exposure in febrile patients during Chikungunya virus introduction in the state of Amapá, Amazon Region, Brazil. *Pathogens* **13**, 469 (2024).
89. Gil-Mora, J. et al. Arbovirus antibody seroprevalence in the human population from Cauca, Colombia. *Am. J. Trop. Med. Hyg.* **107**, 1218–1225 (2022).
90. Ciuoderis, K. A. et al. Oropouche virus as an emerging cause of acute febrile illness in Colombia. *Emerg. Microbes Infect.* **11**, 2645–2657 (2022).
91. Bernardes-Terzian, A. C. et al. Sporadic oropouche virus infection, Acre, Brazil. *Emerg. Infect. Dis.* **15**, 348–350 (2009).
92. Download GADM data (version 4.1). *Global Administrative Areas Database* https://gadm.org/download_country.html (2022).
93. Massicotte, P., South, A. & Hufkens, K. rnaturalearth: world map data from Natural Earth. Version 1.2.0 https://cran.r-project.org/web/packages/rnaturalearth/index.html (2025).

Acknowledgements

W.M.d.S. and N.R.F. were supported by Wellcome Trust Digital Technology Development Award in Climate Sensitive Infectious Disease Modelling (no. 226075/Z/22/Z) and the Wellcome Trust Dengue and Zika Immunology and Genomics Multi-Country Network (DeZi Network; no. 316633/Z/24/Z). J.L.P.-M. is supported by São Paulo Research Foundation (no. 2022/10442-0), National Council for Scientific and Technological Development (CNPq, no. 309971/2023-3). E.R.M. is affiliated with the Wellcome Trust-funded Centres for Antimicrobial Optimization Network (no. 226693/Z/22/Z). V.S.S. was supported by a CNPq fellowship. We acknowledge funding from the MRC Centre for Global Infectious Disease Analysis (no. MR/R015600/1), jointly funded by the UK Medical Research Council and the UK Foreign, Commonwealth and Development Office, under the MRC/FCDO Concordat agreement, and also part of the EDCTP2 program supported by the European Union. A.I.B. was supported by Cornell Atkinson Center seed funding. We thank J. A. Tida (www.plotmyscience.com) for figure editing.

Author contributions

W.M.d.S., J.L.P.-M. and E.C.S. conceptualized the study. E.R.M., X.H., G.C.S., J.F., I.M.C., G.M.P., L.S., A.C.B., C.F.R., N.B.S.B., S.T.S.d.L., R.d.J., R.B.K., B.B.S., C.M.L.S., N.C.P., V.S.S., R.S.R., P.J.L., A.G.C., J.L.P.-M., E.C.S. and W.M.d.S. contributed to the acquisition of data. X.H., G.C.S., O.C.-A., O.R. and W.M.d.S. contributed to the data analysis. X.H., G.C.S., N.R.F., S.C.W., H.S., J.L.P.-M., E.C.S. and W.M.d.S. contributed to data interpretation. W.M.d.S. and X.H. drafted the paper. X.H., G.C.S., L.S., M.P.C., R.S., O.R., A.I.B., N.R.F., S.C.W., H.S., A.G.C., J.L.P.-M., E.C.S. and W.M.d.S. revised the paper. A.G.C., J.L.P.-M., E.C.S. and W.M.d.S. acquired funding for the study. All authors read and approved the final version of the paper and the submission. X.H. and W.M.d.S. accessed and verified all the data reported in the study.

Competing interests

A.C.B., C.F.R. and N.B.S.B. are employees of EUROIMMUN Brasil. The other authors declare no competing interests.

Additional information

Extended data is available for this paper at https://doi.org/10.1038/s41591-026-04221-z.

Supplementary information The online version contains supplementary material available at https://doi.org/10.1038/s41591-026-04221-z.

Correspondence and requests for materials should be addressed to José Luiz Proenca-Modena, Ester C. Sabino or William M. de Souza.

Peer review information *Nature Medicine* thanks Jonas Schmidt-Chanasit, Joseph Wu and the other, anonymous, reviewer(s) for their contribution to the peer review of this work. Peer reviewer reports are available. Primary Handling Editor: Lia Parkin, in collaboration with the *Nature Medicine* team.

https://doi.org/10.1038/s41591-026-04221-z

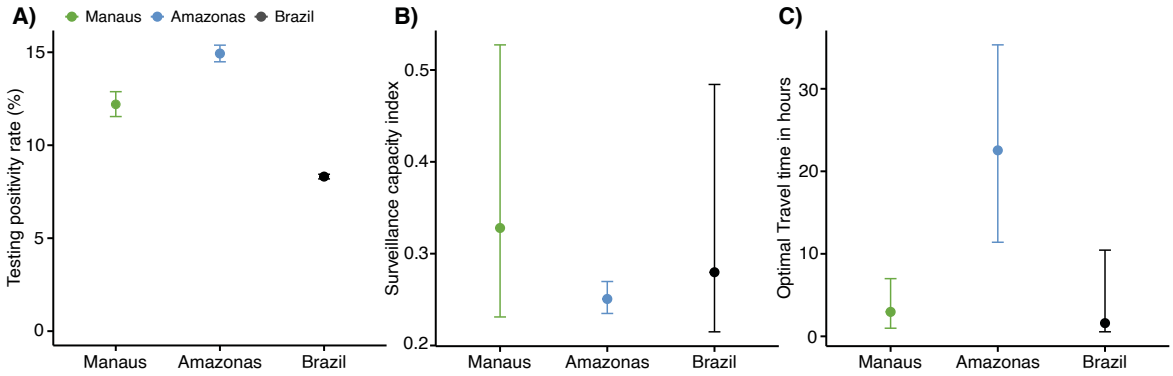

Extended Data Fig. 1 | Testing positivity rates and healthcare access in Manaus, Amazonas, and Brazil. A) Testing positivity rates of Oropouche virus (OROV) for collected samples in 2023 and 2024. Observed rates are shown as dots, and 95% confidence intervals are shown as bars. Data are presented for Manaus (n = 9,345), Amazonas (n = 24,614), and Brazil (n = 187,320). **B)** Model-predicted relative surveillance capacity index for emerging acute viral infectious diseases. The index ranges from 0 (lowest) to 1 (highest). Data are represented as medians (dots) with interquartile ranges (bars). **C)** Optimal travel time to healthcare facilities in hours via motorized transport. Data are represented as medians (dots) with interquartile ranges (bars).

https://doi.org/10.1038/s41591-026-04221-z

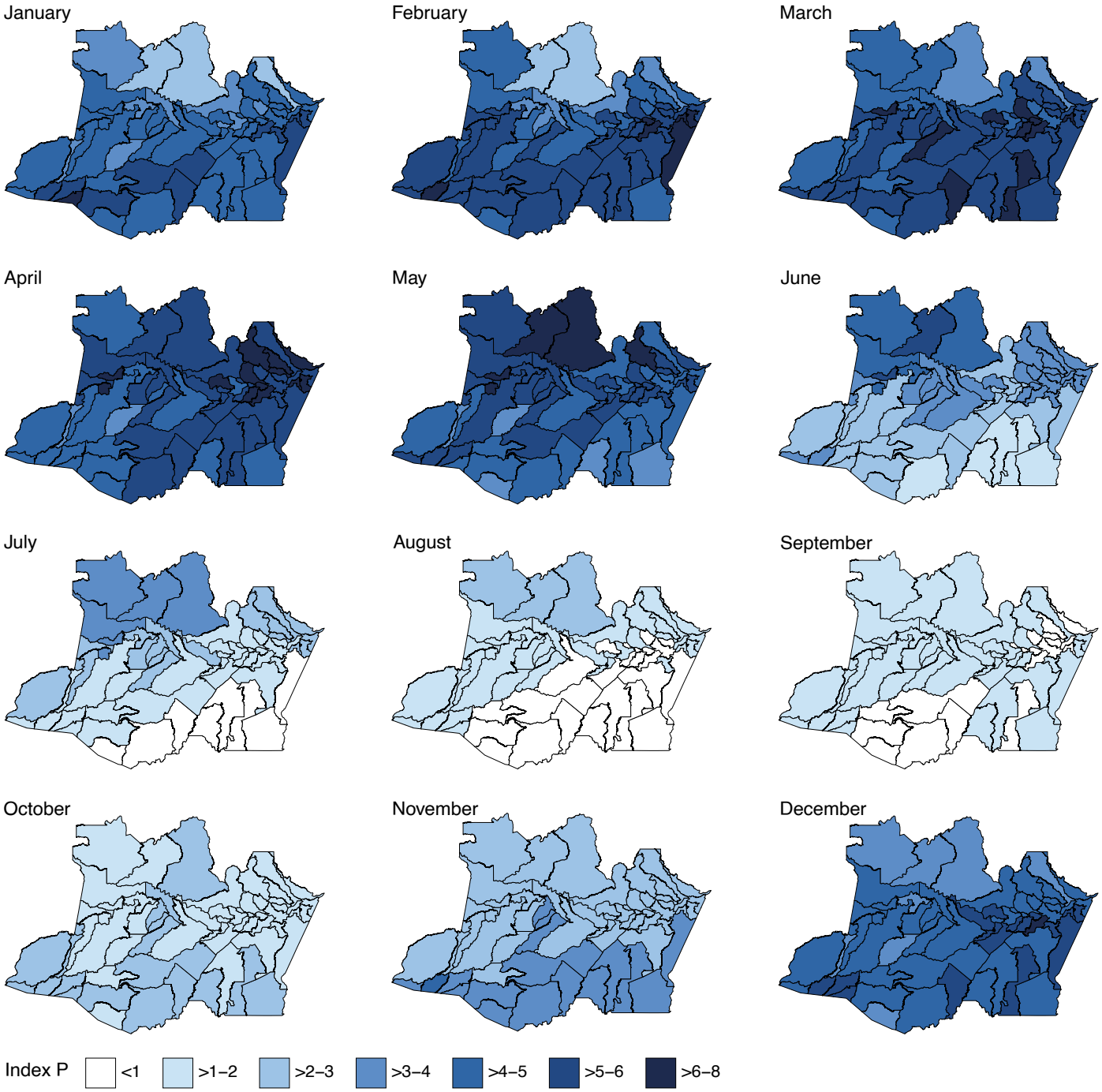

Extended Data Fig. 2 | Spatiotemporal variation in OROV transmission suitability in Amazonas state, Brazil. Mean monthly OROV transmission suitability (Index P) for *Culicoides paraensis* from 2014 to 2024 at the municipality level in Amazonas state. Index P values of ≥1 indicate suitable climate conditions for transmission, and values of <1 indicate unsuitable conditions.

https://doi.org/10.1038/s41591-026-04221-z

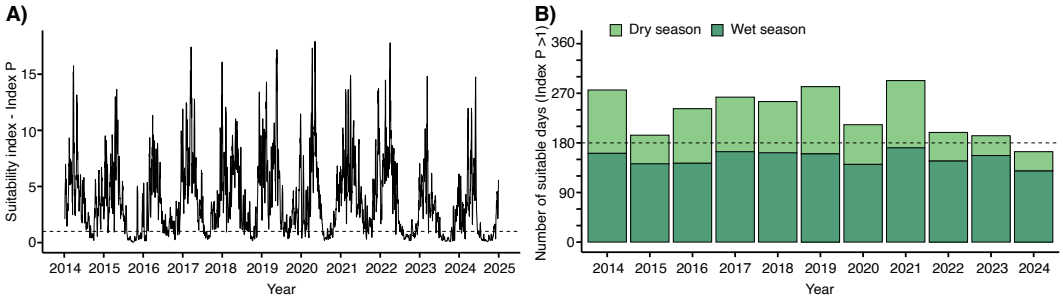

Extended Data Fig. 3 | OROV transmission suitability in Manaus City, Brazil. **A)** Time series of average weekly index P from 2014 to 2025 in Manaus city, Brazil. The dashed line shows that Index P ≥ 1, which indicates a suitable climate for OROV transmission by *C. paraensis*. **B)** The number of days suitable for OROV transmission by *C. paraensis* per year from 2014 to 2024. The dashed line indicates 6 months of suitable climate for OROV transmission by *C. paraensis* for the year.

https://doi.org/10.1038/s41591-026-04221-z

Extended Data Table 1 | Prior distributions used in the MVSE package for estimating the OROV transmission potential via the vector *Clicoides paraensis* midges. N/A

Parameter	Mean	Standard deviation	Distribution	Ref.
Adult *Culicoides* lifespan	15 days	3 days	Normal	36
Extrinsic incubation period	7 days	1 day	Normal	48
Female *Culicoides* feeding frequency	0.25 times per day	0.05 times per day	Normal	49
Human lifespan in Brazil	76.4 years old	2 years	Normal	50
Intrinsic incubation period	9.7 days	1.43 days	Normal	51
Human infectiousness period	3.2 days	0.36 days	Normal	51
Human to vector probability of transmission	0.15% per bite	0.04% per bite	Normal	52

https://doi.org/10.1038/s41591-026-04221-z

Extended Data Table 2 | Seroprevalence by age group for serosurveys conducted in Manaus during 2015 and 2016, November 2023, June, and November 2024

Study	Age group	Mean sample age	Observed seroprevalence	Lower 95% CI	Upper 95% CI
November 2023 (n=685)	16-19	18.44	0.0294	0.0007	0.1533
	20-29	24.26	0.0657	0.0305	0.1210
	30-39	34.97	0.1132	0.0739	0.1638
	40-49	44.12	0.1010	0.0616	0.1525
	50-59	53.68	0.2128	0.1351	0.3093
	60-69	62.05	0.2632	0.0915	0.5120
June 2024 (n=685)	16-19	18.66	0.1143	0.0320	0.2674
	20-29	24.41	0.1648	0.1219	0.2154
	30-39	34.80	0.1889	0.1345	0.2538
	40-49	43.98	0.2044	0.1403	0.2817
	50-59	54.41	0.1724	0.0859	0.2943
	60-69	62.00	0.2143	0.0466	0.5080
November 2024 (n=685)	16-19	18.41	0.2500	0.1146	0.4341
	20-29	24.55	0.2009	0.1510	0.2587
	30-39	34.20	0.2865	0.2237	0.3560
	40-49	44.25	0.2583	0.1906	0.3357
	50-59	54.21	0.2879	0.1830	0.4125
	60-69	62.13	0.6000	0.3229	0.8366
Manaus 2015-2016 (n=314*)	14-19	17.88	0.0606	0.0074	0.2023
	20-29	24.61	0.0152	0.0004	0.0816
	30-39	34.63	0.0526	0.0145	0.1293
	40-49	44.22	0.2308	0.1353	0.3519
	50-59	54.04	0.2292	0.1203	0.3731
	60-69	63.62	0.1905	0.0545	0.4191
	≥70	74.40	0.2000	0.0051	0.7164

Footnote: Excluding 115 negative and 11 positive samples without age data.

https://doi.org/10.1038/s41591-026-04221-z

Extended Data Table 3 | $PRNT_{50}$ titers in OROV antibody-positive samples against OROV AM0088 isolate

	Donation ($PRNT_{50}$ titer)	
Sample ID	**First**	**Second**
AMBD4503	40	640
AMBD7903	640	640
AMBD2203	640	640
AMBD6003	640	640
AMBD6503	Below LOD	320
AMBD9303	40	640

Footnote: LOD, limit of detection.

https://doi.org/10.1038/s41591-026-04221-z

Extended Data Table 4 | Major OROV outbreaks documented from 1961 to 2021

Outbreak No.	County	State	Location	Year	Month	Length Outbreak	Ref.
1	Brazil	Pará	Belém	1961	Feb to May	3	55-57
2	Brazil	Pará	Bragança	1967	Mar to Jul	4	55,57
3	Brazil	Pará	Belém	1968	Feb to Jul	5	55,57
4	Brazil	Pará	Baiao	1972	Jun to Sep	3	55
5	Brazil	Pará	Alter-do-Chão	1975	Jul to Aug	1	55
5	Brazil	Pará	Itupiranga	1975	May to Jun	1	55
5	Brazil	Pará	Mojui dos Campos	1975	Dec to Apr	4	55
5	Brazil	Pará	Belterra	1975	Apr to Jun	2	55
5	Brazil	Pará	Santarém	1975	Apr to Jul	3	58
6	Brazil	Pará	Tomé-Açu	1978	Jul to Sep	2	59
6	Brazil	Pará	Quatro Bocas	1978	Jul to Sep	2	59
7	Brazil	Pará	Belém	1979	Apr to Jun	2	57,60
7	Brazil	Pará	Castanhal	1979	Jul	1	61
7	Brazil	Pará	Capanema	1979	Jul	1	61
7	Brazil	Pará	Caraparu	1979	Mar to Apr	1	61
7	Brazil	Pará	Abaetetuba	1979	Mar to Apr	1	61
7	Brazil	Pará	Santa Izabel do Pará	1979	Mar to Jun	3	61
7	Brazil	Pará	Benevides	1979	Mar to Jun	3	61
7	Brazil	Pará	Ananindeua	1979	Nov	1	61
8	Brazil	Amazonas	Barcelos	1980	May to Jun	1	25
8	Brazil	Pará	Belém	1980	Feb to Oct	8	57,60
8	Brazil	Pará	Augusto Correa	1980	Mar to Aug	5	57
8	Brazil	Pará	Bragança	1980	Mar to Aug	5	57
8	Brazil	Pará	Abaetetuba	1980	Mar to Aug	5	57,60
8	Brazil	Pará	Benfica	1980	Mar to Aug	5	57,60
8	Brazil	Pará	Benevides	1980	Mar to Aug	5	57,60
8	Brazil	Pará	Santa Izabel do Pará	1980	Mar to Aug	5	57,60
8	Brazil	Pará	Castanhal	1980	Mar to Aug	5	57,60
8	Brazil	Pará	Capanema	1980	Mar to Aug	5	57,60
8	Brazil	Amapá	Mazagão	1980	unk	unk	57,60
8	Brazil	Amazonas	Manaus	1980–1981	Oct to Mar	5	25
9	Brazil	Maranhão	Porto Franco	1987–88	Dec to Mar	3	57,62
9	Brazil	Maranhão	Estreito	1987–88	Dec to Mar	2	63
10	Brazil	Tocantins	Tocantinópolis	1988–89	Dec to Mar	2	57,62
11	Panama	Panamá Oeste	Bejuco	1989	Sep	1	57
11	Panama	Panama	Chame	1989	Sep	1	60
11	Panama	Panamá Province	San Miguelito	1989	Sep	1	60
11	Panama	Panamá Province	Chilibre	1990	unk	unk	60
12	Brazil	Rondônia	Ouro Preto do Oeste	1991	Jan to Apr	3	57,62
12	Brazil	Rondônia	Ariquiemes	1991	Jan to Apr	3	57,62
12	Brazil	Pará	Santa Izabel do Pará	1991	unk	unk	57,64
13	Peru	Loreto	Iquitos	1992	Jan to Apr	3	60,65
14	Peru	Madre de Dios	unk	1994	unk	unk	7
15	Brazil	Pará	Curionópolis	1994	Nov to Dec	1	64
16	Brazil	Amazonas	Novo Airão	1996	Mar to May	2	57,63
17	Brazil	Pará	Brasil Novo	1996	Jan to Feb	1	57
17	Brazil	Pará	Vitória do Xingu	1996	Jun to Jul	1	57
17	Brazil	Pará	Oriximiná	1996	Apr to May	1	57,63
17	Brazil	Pará	Altamira	1996	Feb to Jun	4	63
17	Brazil	Acre	Xapuri	1996	Mar to Apr	1	57,63
18	Peru	Loreto	Iquitos	2002	unk	unk	66
19	Brazil	Pará	Parauapebas	2003	Apr to May	1	67
20	Peru	Loreto	Iquitos	2003	unk	unk	66
21	Brazil	Pará	Porto de Moz	2004	Jul to Aug	1	67
22	Peru	Loreto	Iquitos	2004	unk	unk	66
23	Peru	Loreto	Iquitos	2005	unk	unk	66
24	Brazil	Pará	Magalhães Barata	2006	Apr to Aug	4	68
24	Brazil	Pará	Maracanã	2006	Apr to Aug	4	68
25	Peru	Loreto	Iquitos	2006	unk	unk	66
25	Peru	Loreto	Iquitos	2007	unk	unk	66
26	Brazil	Amapá	Mazagão	2009	Jun to Oct	4	7,69
27	Peru	San Martín	Tarapoto	2010	unk	unk	70
27	Peru	San Martín	Bagazán	2010	May	1	71
28	Peru	Cajamarca	Casa Blanca	2011	unk	unk	72
29	Peru	Cusco	Lares	2016	Jan to Mar	2	73
29	Peru	Cusco	Palma Real	2016	Jan to Mar	2	73
29	Peru	Cusco	Quellouno	2016	Jan to Mar	2	73
29	Peru	Cusco	Kimbiri	2016	Jan to Mar	2	73
29	Peru	Cusco	Quebrada Honda	2016	Jan to Mar	2	73
29	Peru	Calca	Yanalite	2016	Jan to Mar	2	73
29	Peru	Cusco	Yuveni	2016	Jan to Mar	2	73
29	Peru	Cusco	Echarate	2016	Jan to Mar	2	73
29	Peru	Calca	Lares	2016	Jan to Mar	2	73
29	Peru	Cusco	Pichari	2016	Jan to Mar	2	73
29	Peru	Huánuco	Huánuco	2016	Jan to Jul	6	74
29	Peru	Madre de Dios	Puerto Maldonado	2016	unk	unk	75
29	Peru	Madre de Dios	unk	2015-16	Dec to Jan	1	75
30	Peru	Piura	Piura	2016	Feb to Jul	5	76
31	Brazil	Pará	Santa Bárbara do Pará	2018	Jan to Feb	1	95
32	French Guiana	–	Saül	2021	Aug to Sep	1	78

Footnote: Abbreviation used: unk = unknown.

nature portfolio

Corresponding author(s): William M. de Souza

Last updated by author(s): Dec 23, 2025

Reporting Summary

Nature Portfolio wishes to improve the reproducibility of the work that we publish. This form provides structure for consistency and transparency in reporting. For further information on Nature Portfolio policies, see our Editorial Policies and the Editorial Policy Checklist.

Statistics

For all statistical analyses, confirm that the following items are present in the figure legend, table legend, main text, or Methods section.

n/a	Confirmed
☐	☒ The exact sample size (*n*) for each experimental group/condition, given as a discrete number and unit of measurement
☐	☒ A statement on whether measurements were taken from distinct samples or whether the same sample was measured repeatedly
☐	☒ The statistical test(s) used AND whether they are one- or two-sided *Only common tests should be described solely by name; describe more complex techniques in the Methods section.*
☒	☐ A description of all covariates tested
☐	☒ A description of any assumptions or corrections, such as tests of normality and adjustment for multiple comparisons
☐	☒ A full description of the statistical parameters including central tendency (e.g. means) or other basic estimates (e.g. regression coefficient) AND variation (e.g. standard deviation) or associated estimates of uncertainty (e.g. confidence intervals)
☐	☒ For null hypothesis testing, the test statistic (e.g. *F*, *t*, *r*) with confidence intervals, effect sizes, degrees of freedom and *P* value noted *Give P values as exact values whenever suitable.*
☐	☒ For Bayesian analysis, information on the choice of priors and Markov chain Monte Carlo settings
☒	☐ For hierarchical and complex designs, identification of the appropriate level for tests and full reporting of outcomes
☒	☐ Estimates of effect sizes (e.g. Cohen's *d*, Pearson's *r*), indicating how they were calculated

Our web collection on statistics for biologists contains articles on many of the points above.

Software and code

Policy information about availability of computer code

Data collection

The datasets used in this study include:
1. Individualized data from four serosurveys (2015-2016, November 2023, June 2024, and November 2024) in Manaus City, Manaus. This dataset includes age, serostatus for Oropouche virus (OROV), neutralization antibody level against OROV (for a subset of samples).
2. Publicly available dataset of OROV infection seroprevalence and outbreaks derived from a literature review (Table S4 and S5).
3. Public health surveillance data from the Brazilian Ministry of Health from January 2014 to January 2025.
4. Population data for Brazil at the municipal, state, and national levels from the 2022 Brazil Census.
5. Population data from Barbados, Bolivia, Colombia, Cuba, Dominican Republic, Ecuador, French Guiana, Guyana, Panama, Peru, Suriname, and Venezuela obtained in the national census.
6. Brazilian municipal-level GIS shapefiles from the Brazilian Institute of Geography and Statistics.
7. Remote sensing data for 2m temperature and 2m dewpoint temperature (2014-2025) from the "ERA5 hourly data on single levels from 1940 to present" published on the Climate Data Store.

Data analysis

All statistical computing analyses were conducted using the RStudio project (version R 4.4.1). R packages necessary for analysis and visualization include: readxl (version 1.4.3), openxlsx (version 4.2.6.1), tidyverse (version 2.0.0), dplyr (version 1.1.4), tidyr (version 1.3.1), scales (version 1.3.0), lubridate (version 1.9.3), raster (version 3.6-26), sf (version 1.0-16), terra (version 1.8-42), tmap (version 3.3-4), ggplot2 (version 3.5.1), ggbreak (version 0.1.2), ggpubr (version 0.6.0), stringr (version 1.5.1), MVSE (version 1.0), and Rsero (version 2.0). No custom code was developed.

For manuscripts utilizing custom algorithms or software that are central to the research but not yet described in published literature, software must be made available to editors and reviewers. We strongly encourage code deposition in a community repository (e.g. GitHub). See the Nature Portfolio guidelines for submitting code & software for further information.

Data

Policy information about availability of data

All manuscripts must include a data availability statement. This statement should provide the following information, where applicable:

- Accession codes, unique identifiers, or web links for publicly available datasets
- A description of any restrictions on data availability
- For clinical datasets or third party data, please ensure that the statement adheres to our policy

We have provided all relevant data in the extended data tables. The data used to establish prior distributions for the MVSE package—which estimated OROV transmission potential via the vector Culicoides paraensis midges—are available in Table S1. Tables S3 and S4 list publicly available seroprevalence and outbreak data compiled and used in our study, along with their original article references. Tables S4 and S5 contain the aggregate seroprevalence data stratified by age group performed in our study. All codes and data used to generate the figures in this manuscript are publicly available on GitHub (https://github.com/wmarciel/Oropouche-LAC). De-identified individual-level data from the Brazilian Ministry of Health can be provided for research purposes after approval by a committee on human experimentation (if applicable). This data can be obtained upon request to the corresponding authors (William M. de Souza, wmdesouza@uky.edu; Ester C. Sabino, sabinoec@usp.br, and Jose Luiz Proenca-Modena, jlmodena@unicamp.br). The estimated response time from the corresponding authors may be up to three weeks.

Research involving human participants, their data, or biological material

Policy information about studies with human participants or human data. See also policy information about sex, gender (identity/presentation), and sexual orientation and race, ethnicity and racism.

Reporting on sex and gender	In our serological surveys, records about sex were derived from participant self-report. No sex-gender specific variables were used in our study.
Reporting on race, ethnicity, or other socially relevant groupings	This study did not collect or use any socially constructed variables, such as race and ethnicity.
Population characteristics	Age was the only demographic variable used in this study, serving to stratify seroprevalence data and inform age specific parameters for Oropouche virus infection.
Recruitment	We retrospectively tested anonymized serum samples from two distinct cohorts of Manaus residents (2,495 samples). The first cohort comprised residual blood samples from Hemoterapia do Amazonas. We retrieved stored residual laboratory screening samples from routine blood donors in November 2023, June 2024, and November 2024. We selected 2,055 samples (685 x 3 time points) to geographically represent Manaus by using the ZIP codes of blood donors. The second cohort, with 440 participants, consisted of blood samples collected from Manaus residents (general population) between 2015 and 2016, at which time no participants reported any symptoms.
Ethics oversight	All procedures were conducted with the approval of the Ethics Committees of the University of São Paulo (approval number 73030523.6.1001.0068) and the Federal University of Amazonas (approval numbers 5.876.612 and 6.629.451).

Note that full information on the approval of the study protocol must also be provided in the manuscript.

Field-specific reporting

Please select the one below that is the best fit for your research. If you are not sure, read the appropriate sections before making your selection.

☒ Life sciences ☐ Behavioural & social sciences ☐ Ecological, evolutionary & environmental sciences

For a reference copy of the document with all sections, see nature.com/documents/nr-reporting-summary-flat.pdf

Life sciences study design

All studies must disclose on these points even when the disclosure is negative.

Sample size	We retrospectively tested anonymized serum samples from two distinct cohorts of Manaus residents (2,495 samples). The first cohort comprised residual blood samples from Hemoterapia do Amazonas. We retrieved stored residual laboratory screening samples from routine blood donors in November 2023, June 2024, and November 2024. We selected 2,055 samples (685 x 3 time points) to geographically represent Manaus by using the ZIP codes of blood donors. The second cohort, with 440 participants, consisted of blood samples collected from Manaus residents (general population) between 2015 and 2016, at which time no participants reported any symptoms. We did not perform a formal sample size calculation for either cohort. Additionally, we compiled and included seroepidemiological studies for Oropouche virus published between 1960 and 2025. The sample sizes from these seroprevalence studies vary depending on each rationale and available funding.
Data exclusions	No data were excluded from analysis.
Replication	All catalogue numbers and manufacturers for the reagents and kits used in our study are detailed in the Methods section. Datasets necessary

Replication	to reproduce the findings of this study are provided in the Extended Data Tables (S1, S3, S4, and S5). Individualized seroprevalence and neutralizing antibody data will be made available on GitHub following manuscript acceptance. All positive samples from the initial screening with the commercial EUROIMMUN ELISA kits for OROV-specific IgG (Cat. No. EI 2771-9601G) and IgM (Cat. No. EI 2771-9601M) were later confirmed by a gold-standard neutralizing antibody test, either the Focus Reduction Neutralization Test (FRNT) or the Plaque Reduction Neutralization Test (PRNT50). A subset of IgG ELISA-positive (n=376), IgG ELISA-negative (n=274), and all IgG ELISA-borderline (n=31) samples were also tested using an FRNT. The results were reliably reproducible. The agreement between the ELISA and the FRNT was 97.8% (318/325) for IgG-positive samples and 98.5% (270/274) for IgG-negative samples.
Randomization	Randomization did not apply to our study because it was a retrospective analysis of existing samples, and not an interventional study.
Blinding	Blinding did not apply to our study because it was a retrospective analysis of existing samples, and it did not involve any experimental groups or participant allocation.

Reporting for specific materials, systems and methods

We require information from authors about some types of materials, experimental systems and methods used in many studies. Here, indicate whether each material, system or method listed is relevant to your study. If you are not sure if a list item applies to your research, read the appropriate section before selecting a response.

Materials & experimental systems

n/a	Involved in the study
☐	☒ Antibodies
☐	☒ Eukaryotic cell lines
☒	☐ Palaeontology and archaeology
☒	☐ Animals and other organisms
☒	☐ Clinical data
☒	☐ Dual use research of concern
☒	☐ Plants

Methods

n/a	Involved in the study
☒	☐ ChIP-seq
☒	☐ Flow cytometry
☒	☐ MRI-based neuroimaging

Antibodies

Antibodies used	Polyclonal anti-OROV antibody (Cat no. VR-1228AF, ATTC, USA) with dilution 1:1000 and anti-mouse IgG secondary antibody (Cat no. AP124P, Sigma-Aldrich, USA) with dilution 1:2000.
Validation	Both commercial antibodies were validated by their manufacturers and were titrated in the lab to determine optimal concentration for experimentation.

Eukaryotic cell lines

Policy information about cell lines and Sex and Gender in Research

Cell line source(s)	Vero CCL81 cells (African green monkey, ATCC no. CCL81) were purchased from American Type Culture Collection (ATCC, Manassas, VA).
Authentication	Vero CCL81 cells were purchased from ATCC. According to ATCC's instructions, this cell line was authenticated using STR profiling before being shipped to us.
Mycoplasma contamination	We periodically tested all cell lines in our lab for mycoplasma contamination using commercial kits, such as the LookOut Mycoplasma PCR Detection Kit (Sigma, MP0035-1KT). All cell lines used in this study were free of mycoplasma.
Commonly misidentified lines (See ICLAC register)	No commonly used misidentified cell lines were used.

Plants

Seed stocks	*Report on the source of all seed stocks or other plant material used. If applicable, state the seed stock centre and catalogue number. If plant specimens were collected from the field, describe the collection location, date and sampling procedures.*
Novel plant genotypes	*Describe the methods by which all novel plant genotypes were produced. This includes those generated by transgenic approaches, gene editing, chemical/radiation-based mutagenesis and hybridization. For transgenic lines, describe the transformation method, the number of independent lines analyzed and the generation upon which experiments were performed. For gene-edited lines, describe the editor used, the endogenous sequence targeted for editing, the targeting guide RNA sequence (if applicable) and how the editor was applied.*
Authentication	*Describe any authentication procedures for each seed stock used or novel genotype generated. Describe any experiments used to assess the effect of a mutation and, where applicable, how potential secondary effects (e.g. second site T-DNA insertions, mosiacism, off-target gene editing) were examined.*